INSTITUTO UNIVERSITÁRIO EGAS MONIZ

MESTRADO EM TECNOLOGIAS LABORATORIAIS EM CIÊNCIAS FORENSES

PHYTOCANNABINOID EFFECT ON ALPHA-SYNUCLEIN AGGREGATION

Trabalho submetido por
João Serra Velez
para a obtenção do grau de Mestre em Tecnologias Laboratoriais em Ciências Forenses

novembro de 2022

INSTITUTO UNIVERSITÁRIO EGAS MONIZ

MESTRADO EM TECNOLOGIAS LABORATORIAIS EM CIÊNCIAS FORENSES

PHYTOCANNABINOID EFFECT ON ALPHA-SYNUCLEIN AGGREGATION

Trabalho submetido por
João Serra Velez
para a obtenção do grau de **Mestre** em Tecnologias Laboratoriais em Ciências Forenses

Trabalho orientado por
Prof. Doutor Alexandre Luís de Matos Botica Côrtes Quintas
e coorientado por
Mestre Carla Filipa da Silva Ferreira

novembro de 2022

To my parents,
my sister Madalena
and my brother Tomás,
to Carolina and her
family.

Acknowledgements

To Prof. Doutor Alexandre Quintas and Mestre Carla Ferreira for believing in me to carry out this experiment, helping me in every situation I needed and providing suggestions to improve every day, helping me becoming a better scientist.

To my parents, for nourishing my passion for science since an early age, pushing me to read books and replying to all my questions, for always trusting me and help me fight to achieve my dreams.

To my brother Tomás and my sister Madalena, my partners in crime, the ones that always make me realise how much of a responsibility it is to be the older brother and lead by example.

To my best friends João, Chico and Gui who have always pushed me to be better, pointing my flaws and helping me to improve myself, emotionally, personally, and socially.

To Carolina, for helping me understand how people with different views of the world can become an unstoppable force when working together, for lifting me up when I was going down and help me to thrive no matter the circumstance.

To Catarina, who helped me value the work of teacher even more than I already did, for showing me that watching someone getting better at what they love in matter of weeks is truly fascinating.

To Daniela and Rafael, for being always happy to help and becoming my early morning and late evening companions.

To my colleagues, Ana, Daniela, Filipa, Joana, Raquel, Rita, and Vlad, for all the point of view exchanges, the discussions, the debates, the laughs, and all in between.

To Miguel and Ricardo, the boys of the class who helped me feeling at home since day 1 and became my closest friends during this journey.

To everyone who was part of my academic journey so far.

Nothing is true, everything is permitted.

Declaração de Honra

Certifico que sou responsável pelo trabalho submetido neste relatório e que o trabalho é original, não sendo copiado ou plagiado de outra fonte, excetuando o especificado nas referências. Adicionalmente, declaro que o trabalho em si contido não foi submetido anteriormente para qualquer outro propósito.

Monte da Caparica, 29 de novembro de 2022

_____

João Velez

Resumo

A Doença de Parkinson é uma doença em crescimento rápido em termos de prevalência, em especial na última geração. Os sintomas da Doença de Parkinson estão geralmente associados com debilidades no sistema motor. Os corpos de Lewy são maioritariamente aceites pela comunidade científica como um marcador da Doença de Parkinson. Os corpos de Lewy são maioritariamente compostos por α-sinucleína. De acordo com a literatura, a formação de oligómeros de α-sinucleína devido a alterações no enrolamento de folhas-β, vistas em fibras amilóides, é a hipótese atualmente aceite em relação ao aumento das patologias de Lewy e as suas representações neurodegenerativas. A cannabis é utilizada por doentes com Parkinson para reduzir os sintomas. Estudos recentes indicam que o efeito dos fitocanabinóides são mediados pelos receptores CB1 e/ou CB2. O presente estudo tem como objetivo perceber as interações entre a α-sinucleína e o canabidiol, através do estudo do comportamento da α-sinucleína em solução. Depois da purificação da α-sinucleína, esta foi incubada com canabidiol (CBD) e o seu perfil oligomérico, nível de agregação e estrutura secundária através de cromatografia de exclusão molecular, espetroscopia de fluorescência com ThT e dicroísmo circular. Os resultados da cromatografia por exclusão molecular revelaram um equilíbrio entre o dímero e o tetrâmero, com um aumento do dímero na amostra com CBD. No dicroísmo circular, a percentagem de *random coil* diminuiu em ambas as amostras. A análise de Tioflavina-T levou à conclusão de que não existiu agregação. No ensaio com menor concentração, na cromatografia de exclusão molecular, existiu um equilíbrio dinâmico entre o dímero e o monómero, que por sua vez se alterou para outra forma monomérica no fim da experiência.

Palavras-chave: Doença de Parkinson, α-sinucleína, canabinoides, canabidiol, agregação, cromatografia de exclusão molecular.

Abstract

Parkinson's disease is a fast-growing disease in terms of prevalence, especially in the last generation. The symptoms of PD are usually associated with impairments in motor skills. Lewy bodies are a PD feature widely accepted by the scientific community. The Lewy bodies are mainly composed by α-synuclein (α-syn). According to the literature, the formation of α-syn oligomers due to folding changes forming β-sheets, which are seen in amyloid fibrils structure is the currently accepted hypothesis regarding the rise of the Lewy pathologies and their neurodegenerative roles. Cannabis is used by Parkinson´s Disease patients worldwide to reduce symptoms. Recent studies suggest that the effects of phytocannabinoids are mediated by CB1 and/or CB2 receptors. The present study aimed to understand the interactions between α-synuclein and cannabidiol, by studying the behaviour of α-synuclein in solution when exposed to this phytocannabinoid. After α-synuclein purification, the protein was incubated, with Cannabidiol (CBD) and its oligomeric profile, aggregation rate and secondary structure was assessed by gel exclusion chromatography, ThT fluorescence spectroscopy and circular dichroism. The results from the size-exclusion chromatography reveal an equilibrium between dimer and tetramer, with a higher increase of the dimer in the CBD sample. Regarding the circular dichroism, the percentage of random coil decreased in both samples. The ThT analysis led to the conclusion that there was no aggregation of α-synuclein. At low protein concentration the size-exclusion chromatography revealed a dynamic equilibrium between the dimeric and monomeric species, which in turn change to other monomeric form, appearing in the chromatogram, towards the end of the experiment.

Keywords: Parkinson's Disease, α-synuclein, cannabinoids, cannabidiol, aggregation, size-exclusion chromatography

Table of Contents

Figure Index

Table Index

Abbreviations

α-syn	Alpha-synuclein
Δ8-THC	Delta-8-tetrahydrocannabinol
Δ9-THC	Delta-9-tetrahydrocannabinol
ADP	Adenosine Diphosphate
ATP	Adenosine Triphosphate
ATPase	Adenosine Triphosphatase
BCE	Before Common Era
CB1	Cannabinoid Receptor 1
CB2	Cannabinoid Receptor 2
CBC	Cannabichromene
CBD	Cannabidiol
CBDA	Cannabidiolic acid
CBE	Cannabielsoin
CBG	Cannabigerol
CBL	Cannabicyclol
CBN	Cannabinol
CBND	Cannabinodiol
CBT	Cannabitriol
CD	Circular Dichroism
E. coli	*Escherichia coli*
EOPD	Early-Onset Parkinson's Disease
FDA	Food and Drug Administration of the United Stated of America
HPLC-UV	High-performance liquid chromatography with Ultraviolet
HSF1	Heat shock transcription factor 1
HSP	Heat Shock Protein
Hsp27	Heat Shock Protein 27
Hsp40	Heat Shock Protein 40
Hsp70	Heat Shock Protein 70
Hsp90	Heat Shock Protein 90
IEX	Ion-Exchange Chromatography
IPTG	Isopropyl β-D-1-thiogalactopyranoside
LB	Lysogeny broth
LOPD	Late-onset Parkinson's Disease
MPTP	1-methyl-4-phenyl-1,2,3,6-tetrahydropyridine
MW	Molecular Weight
PD	Parkinson's Disease
PMSF	Phenylmethylsulphonyl fluoride
Rt	Retention Time

SDS-PAGE	Sodium dodecyl-sulfate polyacrylamide gel electrophoresis
SEC	Size-Exclusion Chromatography
ThT	Thioflavin-T

1. Introduction

1.1 Parkinson's Disease

Parkinson's Disease (PD) is a fast-growing disease in terms of prevalence, especially in the last generation (Ferreira *et al.* 2020). It is the most common neurodegenerative diseases, after Alzheimer's Disease (Ferreira *et al.* 2020; Ohgita, 2022, Cooray 2020). The symptoms of PD are usually associated with impairments in motor skills, such as shaking, slower or interrupted movements (bradykinesia), difficulties in locomotion and rigidity though there are other symptoms, not related to motor skill, including depression, loss of smell and taste, constipation, psychosis, anxiety, and cognitive and behavioural disorders which may progress to dementia (Polymeropoulos *et al.*, 1997), Pujols *et al.*, 2020; Mahoney-Sánchez *et al.*, 2021). Even though this disease was once considered to be age-related due to the late onset at around 60 years of age, it is now known that the onset of this disease can be as early as 21 years of age (Ferreira *et al.* 2020). When the onset of PD is comprised between the 21 and 50 years of age, it is considered to be early-onset Parkinson's Disease (EOPD). The onset of PD may be due to genetic and environmental factors, even though the vast majority of cases are sporadic (Ferreira *et al.* 2020). According to the literature, 5% of the PD cases are related to genetic causes. EOPD have a higher chance of being related to genetic factors than the late-onset PD (LOPD) (Ferreira *et al.* 2020). Data from clinical reports are in compliance with the low values for genetic and environmental PD, as most of the cases have an unknown aetiology (Ferreira *et al.* 2020). Studies suggest that associating genetic and environmental factors, such as the consumption of substances, may increase the risk of PD, as the cellular response and the metabolism of substances or toxins may increase the genetic tendency to PD. Chemicals and pollutants like MPTP (1-methyl-4-phenyl-1,2,3,6-tetrahydropyridine) are known to modify the gene expression related to PD, leading to a diminished resistance of neurons to toxins (Ferreira *et al.* 2020).

1.2 Lewy Bodies and α-synuclein

Among the scientific community, the Lewy Bodies are known as being the major pathological hallmark of PD (Shahmoradian *et al.* 2019). The Lewy bodies have α-

synuclein (α-syn) as their main component and this protein has been linked to the formation of other pathologies such as Lewy Neurites (Wegrzynowicz, 2019; Cookson 2009; Yasuda 2012; Shahmoradian *et al.* 2019). According to the literature (Dauer 2003; Mahoney-Sánchez *et al.*, 2021), the formation of α-syn oligomers due to β-sheets abundant in amyloid fibrils, resulting from pathogenic α-syn aggregates is the currently accepted hypothesis regarding the rise of the Lewy pathologies and their neurodegenerative roles. According to Wakabayashi and collaborators. (2012) the A53T variant was identified along with autosomal dominant PD. The development of PD can also be associated with the α-syn gene multiplication and the A30P and E46K missense mutations (Wakabayashi *et al.* 2012). It is accepted by the scientific community that α-syn is one of the principal components of the Lewy Bodies in both sporadic and hereditary PD (Wakabayashi *et al.* 2012). It is believed that there are two types of Lewy Bodies – Brainstem and Cortical. Brainstem Lewy Bodies were microscopically observed and described by Wakabayashi *et al.* (2012) as "intracytoplasmic, single or multiple, spherical or elongated, eosinophilic masses possessing a dense core and a peripheral halo", while the Cortical Lewy Bodies were described as also eosinophilic with the difference that there was no regular shape, the structures were not well defined and often without a visible halo or core. Lewy Neurites are Lewy Bodies that are found in neuronal processes. Structurally, the Brainstem and Cortical Lewy Bodies are similar, mainly composed of thicker neurofilament-like structures. In the core of Brainstem Lewy Bodies, there were observed vesicular structures and abnormal filaments. The existence of the argyrophilic inclusions in the midbrain of PD patients was revealed to be immunoreactive to α-syn. The Lewy Bodies are present throughout the nervous system even though they are more predominant in the substantia nigra (Wakabayashi *et al.* 2012).

Incidental Lewy Body Disease is considered to happen when the presence of Lewy Bodies is detected even though there is no clinically documented PD or dementia in the patient, and it is considered to be a pre-symptomatic stage of PD or Dementia. Braak *et al.* (2003, 2006) suggested a PD evolutionary scheme based in 6 stages, based on the presence of α-syn pathology in the dorsal vagal nucleus and in the olfactory bulb. The scheme suggests an evolution of the presence of α-syn pathologies starting in the dorsal vagal nucleus (stage 1) through the pontine tegmentum (stage 2), passing in the midbrain (stage 3) and the basal forebrain and mesocortex (stage 4) and finally

to the neocortex (stages 5 and 6). According to this scheme the first two stages correspond to Incidental Lewy Body Disease, the stages 3 and 4 are related with motor symptoms and the final stages correspond to cognitive impairment and the maximum severity of this disease.

1.3 Molecular Models in Parkinson's Disease

There are several proposed models to the behaviour of α-syn and its conformational changes in solution. All these models are set under the assumption that α-syn, in its wild-type, is monomeric and evolves towards an oligomeric or aggregated form.

Villar-Piqué *et al.* (2015) suggested a triangle shaped model, being function, structure, and toxicity of α-syn in each of the vertexes. In this model, it is suggested that α-syn evolves from a monomeric state into an oligomeric state and further into aggregates. The aggregation of an oligomer would be determined by the oligomerization process, which could lead to either protofibrils and later into fibrils and aggregates, or functional proteins.

Lashuel and collaborators (2012) (Figure 1) proposed that there is an equilibrium between various types of oligomeric structures, such as spherical or annular oligomers, and the monomeric structure. The authors suggested that this balance leads to the formation of fibrils when the ratio of monomers to other structural types of α-syn is low. Lashuel and collaborators (2012) also stated that the unfolded monomeric structure interacts with the parallel dimers and a dynamic equilibrium is formed. According to the authors, the addition of monomers to the solution will increase the dimers and then cause the formation of oligomers. The prevalence of the oligomeric structure can also grow by the addition of soluble monomers, leading to the formation of small amyloid fibrils and consequently, by build-up, longer fibrils. These fibrils will then lead to the formation of Lewy Bodies (Lashuel *et al.*, 2012).

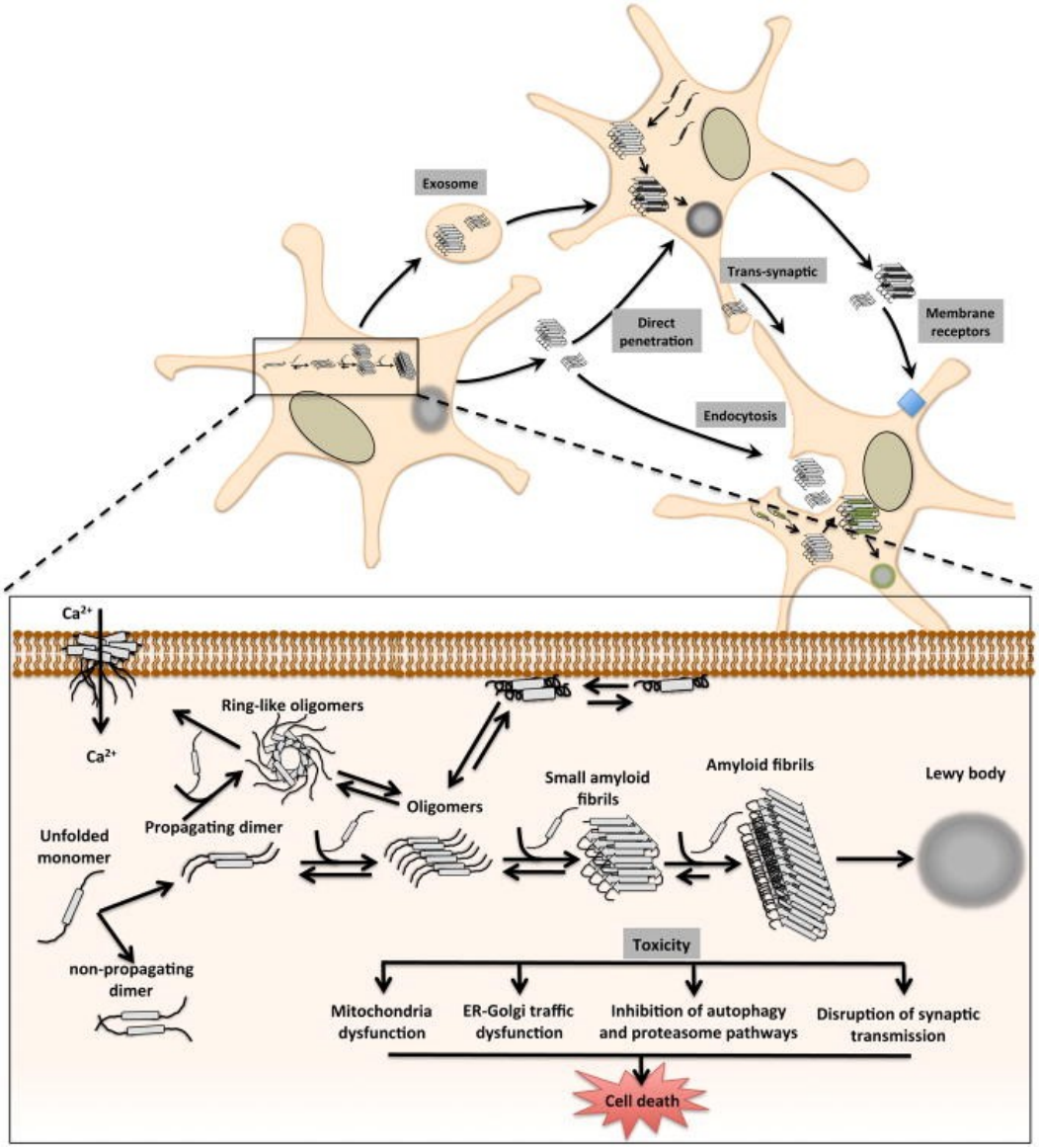

Figure 1 - Suggested model for α-syn aggregation and fibril formation proposed by Lashuel *et al.* (2012)

Mehra *et al.* (2019) (Figure 2) suggests that there are several paths of oligomerization of both wild-type α-syn and mutant α-syn monomers and the type of oligomers formed may be stable on their own, or undergo aggregation into small fibrils, leading to larger fibrils, which can then lead to stable molecules, undergo surface-catalysis or suffer fragmentation, also creating stable oligomers. This group of steady oligomers are the eventual cause of synucleinopathies, such as PD.

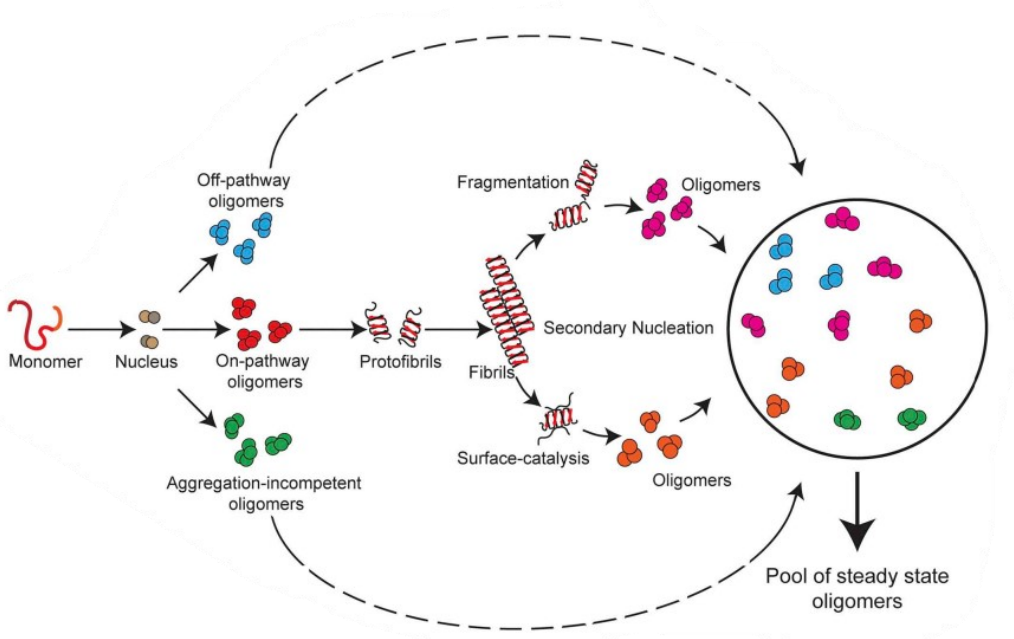

Figure 2 - Suggested model for α-syn aggregation and fibril formation proposed by Mehra *et al.* (2019)

1.4 Chaperones and Chemical Chaperones

Chaperones are a class of small proteins that are responsible for protein homeostasis in all organisms (Dimant *et al.*, 2012). These molecules help in both folding of newly synthesized proteins and in the refolding of partially folded or misfolded proteins (Dimant *et al.*, 2012; Horton *et al.*, 2014). They may also intervene in decision making processes of either refolding a misfolded protein or target it for degradation. The process of degradation has two pathways, being these the ubiquitin-proteasome system or the autophagy-lysosomal pathway (ubiquitin-proteasome system). The actions of molecular chaperones allow proper folding of proteins that would have been misfolded in overcrowded cellular environments (Dimant *et al.*, 2012).

By having the capability of identifying misfolded proteins and preventing protein misfolding, molecular chaperones play a role in PD. Actually, Lewy Bodies reveal the presence of heat shock proteins (HSPs) such as Hsp40, Hsp70 and TorsinA. The presence of these HSPs reveal a molecular attempt to control protein aggregation through molecular chaperones. The up-regulation of Hsp27, Hsp40 and Hsp70 seems to have a direct effect on the regulation of the overexpression of α-syn (St Martin *et al.*, 2007). The inevitable age-related decrease of HSPs capability of controlling protein aggregation may also play a role in the formation of toxic protein inclusions.

This will lead to a compromised ability of the chaperones to regulate the folding issues that may occur. In turn, this series of events, lead to a repetitive loop causing neurodegeneration.

Hsp70 is considered to be the most common response from a protein up-regulation regarding cellular stress, and it has been linked to PD and α-syn as a therapeutic approach. Hsp70 is composed of two domains, being these the N-terminal ATPase domain and the C-terminal ligand binding domain. Even though Hsp70 is active both in the forms bound to ATP and ADP, the ADP form has revealed to have an increased chaperone activity (Dimant *et al.*, 2012). The regulation of Hsp70 comprises several levels of regulation, such as the regulation of transcription and expression of the expressed proteins. Heat shock transcription factor 1 (HSF1) and HSPs form a complex, which is inactive when the cellular stress is inexistent. However, when the cells are subjected to stress conditions, HSF1 is released from the complex, and binds with heat shock elements in the promoter region of HSP gens in order to start the transcription. The function of Hsp70 is also responsible for protein regulation with co-chaperones mediation (Dimant *et al.*, 2012).

There are several studies in which it was demonstrated that Hsp70 is able to regulate the level of α-syn protein aggregation. It was observed that Hsp70 prevented, reduced, and eliminated α-syn oligomers thus decreasing the α-syn toxicity in cells. Klucken *et al.* (2004, 2006) was able to observe that an amino acid substitution in the ATPase binding domain of Hsp70 resulted in an inability to protect against α-syn toxicity. Furthermore, it was also observed that Hsp70 can affect α-syn conformation and disrupt its oligomerization, directly linking the chaperone function of Hsp70 and α-syn aggregation. Another study highlighted that the expression of Hsp70 modified extracellular α-syn aggregates and thus reducing the amount of extracellular α-syn induced toxicity, backing up the role of chaperons in the reduction and clearance of α-syn oligomers (Dimant *et al.*, 2012).

Hsp90 has a similar structure to Hsp70, as it also has an N-Terminal ATPase domain. However, the C-terminal of Hsp90 is responsible for protein dimerization. In patients with PD, Hsp90 was present in filamentous aggregates in Lewy Bodies and Lewy Neurites. Like Hsp70, Hsp90 was found to have an impact in the modulation and clearance of protein inclusions at a cellular level, due to Hsp90's association with α-syn when oxidative stress exists. It was also observed that Hsp90 binds to a region in α-syn, inhibiting the binding to vesicles. Nevertheless, when ATP is present, Hsp90

was observed to be a promoter of α-syn fibril formation. According to Liang *et al.* (2008), Hsp90 has also been linked to the suppression of α-syn's toxicity in yeast models.

Chemical chaperones are small organic molecules with chaperone-like activities. In the 70's a couple of authors observed the effect of alcohol and polyols as protein stabilizers against thermal denaturation (Back et al., 1979). A decade later other authors observed that glycerol facilitate protein folding and correct oligomeric assembly (Lin et al., 1981; Henle *et al. 1983)*. More recently, other small molecules have been suggested as chemical chaperones, such as 4-phenylbarbituric acid, a low molecular weight fatty acid (Rubenstein & Zeitlin, 2000). Overall, small organic molecules may act as protein stabilizers.

1.5 Phytocannabinoids

Cannabis sativa L. is a prevalent species in nature and can thrive in a large number of regions around the globe. The utilization of Cannabis as either a source of food or as a textile fibre (Kriese *et al.*, 2004) can be dated as far back as 5000 years (Farnsworth, 1969, Turner *et al.*, 2017), and its use as a medicinal plant can be traced back to 6th century BCE in the Mesopotamia and in the Nile Delta regions (Thomas & ElSohly, 2016).

The number of natural compounds, cannabinoids and non-cannabinoids of Cannabis have increased from 423 in 1980 to 545 in 2012 (Handbook of Cannabis, 2014). Cannabinoids are a class of substances composed by chemical substances isolated from *Cannabis Sativa L*. and their derivatives, as well as from by-products originating from the plant, called phytocannabinoids (Pertwee, 2009). Until 2014, 104 phytocannabinoids were isolated and grouped into 11 categories, being them delta-9-tetrahydrocannabinol (Δ9-THC) (18 compounds), delta-8 -tetrahydrocannabinol (Δ8-THC) (2 compounds), cannabigerol (CBG) (17 compounds), cannabichromene (CBC) (8 compounds), cannabidiol (CBD) (8 compounds), cannabinodiol (CBND) (2 compounds), cannabielsoin (CBE) (5 compounds), cannabicyclol (CBL) (3 compounds), cannabinol (CBN) (10 compounds), cannabitriol (CBT) (9 compounds), and miscellaneous-type cannabinoids (22 compounds) (Handbook of Cannabis 2014).

CBD and cannabidiolic acid (CBDA) are the major metabolites of the non-psychotropic variety of phytocannabinoids. CBD was isolated from cannabis in the end of the 1930s and beginning of the 1940s, while its structure was explained in 1963 (Handbook of Cannabis. 2014). CBD is considered to have therapeutic potential either as an anti-inflammatory and as a neuroprotector. The Food and Drug Administration of the United States of America (FDA) has already approved Sativex®, which is composed of Δ9-THC and CBD, as a medication to alleviate cancer and multiple sclerosis pains. The therapeutic potential of CBD is related to its ability to target the CB1 and CB2 cannabinoid receptors (Thomas & ElSohly, 2016; Handbook of Cannabis, 2014). However, phytocannabinoids were never tested as chemical chaperones. In the present dissertation, a step is given to understand the potential of phytocannabinoids as chemical chaperones.

2 Materials and Methods

2.1 Culture, Expression and Lysis

A colony of *Escherichia coli (E. coli)* transformed with pt7-7-*SNCA* was inoculated in Lysogeny Broth (LB) with 50µg/ml of ampicillin. The inoculum was incubated overnight at 37ºC with agitation. After incubation, cultures were performed and left incubating at 37ºC with agitation until the Optical Density at 600nm reaches 0,45 nm. 1mM of Isopropyl β-D-1-thiogalactopyranoside (IPTG) was added to the culture and left incubating for 6h at 37ºC with agitation. After incubation, the whole culture was centrifuged at 9500rpm for 5 mins. The supernatant was discarded and 6ml of the lysis buffer were added to the falcons. The lysis buffer consists of 50mM Tris (pH 8,5), 50mM KCl, 50mM MgAc, 0,1% (w/v) NaN_3 and 300mM Phenylmethylsulphonyl fluoride (PMSF). The falcon tubes were then stored at -80ºC after homogenization.

2.2 Extraction

Following the defrosting of the falcon tubes, the samples were sonicated and then divided into ultracentrifuge tubes. The tubes were then ultracentrifuged at 14500 rpm for 30 mins in a Beckman Coulter Optima™ Ultracentrifuge LE-80k. After the ultracentrifugation, the supernatant was boiled in a bain-marie for 20 mins. The samples were again distributed into the ultracentrifuge tubes and ultracentrifuged at 22900 rpm for 40 mins. The supernatant was then filtered using a 0,2 µm cellulose filter. The samples were then stored at -80º C until the purification.

2.3 Ion-Exchange Chromatography (IEX)

The samples were injected into an IEX Column (Q Sepharose™). The mobile phase was a gradient system consisting of (A) 20mM Tris (pH=8) and (B) 20 mM Tris 0,75 M NaCl (pH = 8) (with an increase of 1,11% of buffer B every minute after the first 30 mins with 100% of the buffer A working at 5ºC with a flow rate of 1,5 mL/min. The protein corresponding to the chromatographic peaks at retention times 135 to 165

mins were collected in falcon tubes and confirmed by SDS-PAGE. The samples were stored at -80ºC and then lyophilized.

2.4 *Size-Exclusion Chromatography (SEC)*

After lyophilization, the content of each falcon was dissolved in 1,25 ml of ultrapure water. The samples were then run through a Superdex 75 column with a 150mM Ammonium Bicarbonate (pH = 7,5) at temperature of 5ºC and a flow rate of 1mL/min using a HPLC-UV pump (Jasco PU 2080/ UV 2075). The samples were collected and tested for α-synuclein by SDS-PAGE, stored at -80ºC and then lyophilized. The lyophilized samples that contained α-synuclein were then injected into a Superdex 200 with a buffer of 50mM sodium phosphate buffer (pH = 7,4) using a HPLC-UV pump (Jasco PU 2080/ UV 2075) at a flow rate of 0,4 ml/min and the retention time was compared to the calibration curve. The α-synuclein peak was collected and quantified for the amount of protein present by spectrophotometer, and then was diluted to 46 μM prepared for incubation with CBD.

2.5 *Incubation with CBD*

For each assay, two samples were prepared, one containing α-synuclein (control sample) and one containing 1,5724 mg/ml CBD and 0,66 mg/ml α-synuclein. Both samples were then incubated at 37ºC at 400 rpm (Eppendorf 13-175 Thermomixer compact) and aliquots of each were collected at different time stamps and used to analyse the concentration of the protein, secondary structure conformation and aggregation.

2.6 *Size-Exclusion Chromatography Analysis*

The samples from the aliquots were injected into a Superdex 200 with the same conditions described above.

2.7 Circular Dichroism

The samples were analysed by Circular Dichroism (170 to 280nm) in a spectropolarimeter (Jasco-180). 40µL aliquots were placed in a 0,1mm cell. The circular dichroism spectra were deconvoluted using the CONTIN algorithm with the reference set 6 in the DichroWeb Analyser. (Miles *et al.*, 2021; Sreerama *et al.* 2000; van Stokkum, 1990)

2.8 Thioflavin-T

A 10 mM ThT stock solution was prepared and diluted to 500 µM with 50 mM of sodium phosphate buffer (pH = 7,4). The samples preparation consisted of 20 µL 500 µM ThT, 10 µL of the sample and 200 µL of buffer. The fluorescence was measured using a spectrofluorometer (Perkin Elmer LS50B) in the range of 460 to 560 nm, with an excitation wavelength of 450 nm and the value at 482 nm (maximum fluorescence) was recorded.

3 Results and Discussion

3.1 Behaviour of α-syn in solution

A calibration curve (Figure 3) was created using a combination of the MWGF200 and the MWGF70 Sigma Aldrich Marker Kits in order to establish the retention time of the subspecies of α-syn. The substances with the known molecular weight used to create this curve were β-Amylase from sweet potato (MW=200000 Da), Alcohol Dehydrogenase from yeast (MW=150000 Da), Albumin from bovine serum (MW=66000 Da), Carbonic Anhydrase from bovine erythrocytes (MW=29000 Da), Cytochrome C from horse heart (MW=12400 Da) and Aprotinin from Bovine lung (MW=6500 Da). From this calibration curve, the retention time of the α-syn monomer, dimer and tetramer were calculated.

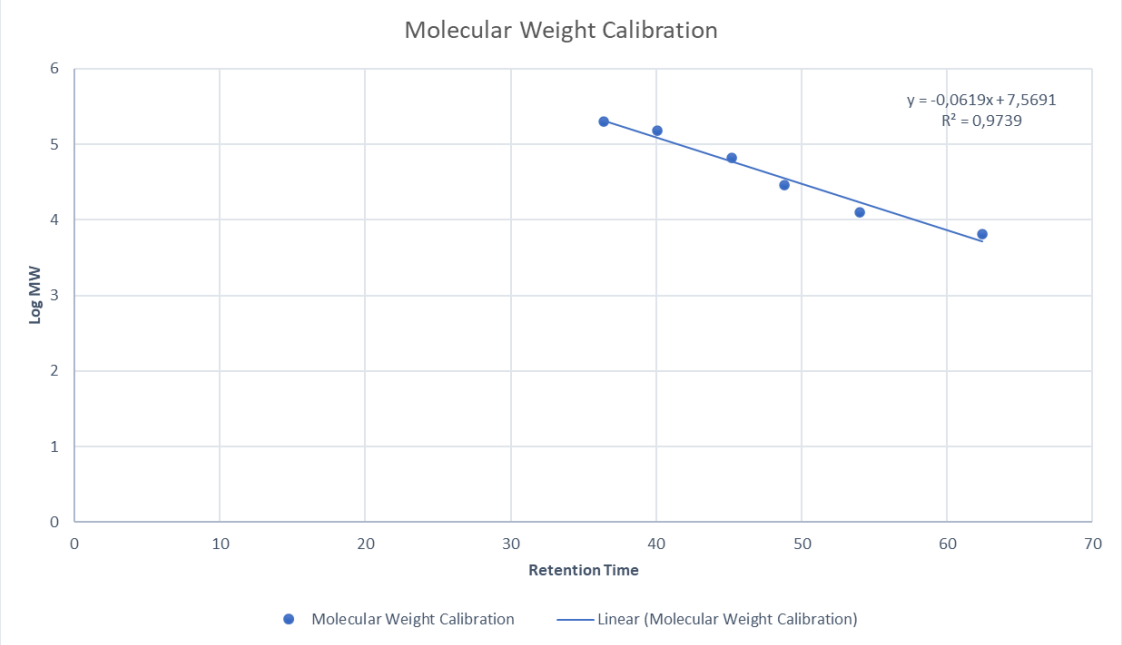

Figure 3 - Calibration Curve for the molecular weight of subspecies of α-syn

Applying the equation resulting from the trendline of the calibration curve, the retention time expected for the α-syn monomer (MW = 14460 Da) would be around 55,072 minutes, for the dimer (MW = 28920 Da) would be around 50,209 minutes and for the tetramer (MW = 57840 Da) would be around 45,345 minutes.

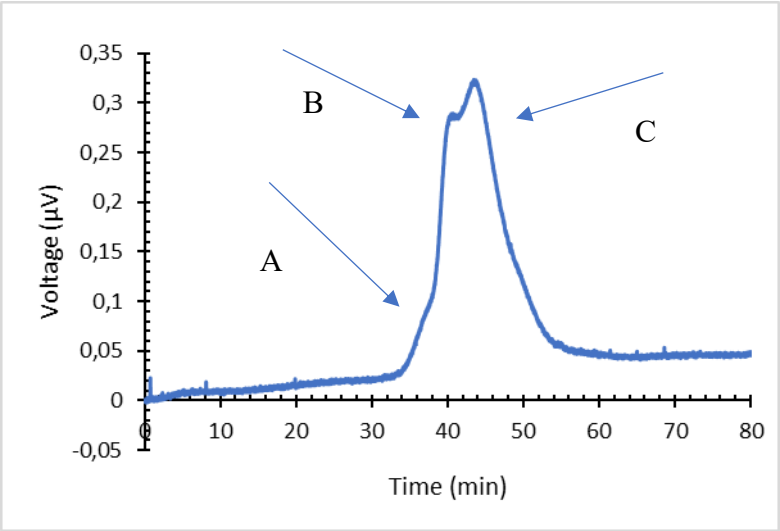

Figure 4 - Chromatography results of α-syn in solution (0,66mg/ml) at T0. **(A)** corresponds to the oligomer, **(B)** corresponds to the tetramer and **(C)** corresponds to the dimer

Analysing the chromatogram in figure 4 we can observe that the tallest part of the mixed peak, around the 45-minute mark, corresponds to the tetramer (MW = 60000 Da), according to calibration curve values mentioned before. The smallest part of the mixed peak, around the 40-minute mark, represents an oligomer around double the size of the tetramer. The 36-minute marks a small variation in the peak can also be observed and it indicates the presence of a molecule of higher molecular weight. Furthermore, between the 50-minute mark, another variation can also be observed in the slope of the peak, most likely indicating the presence of a dimeric structure.

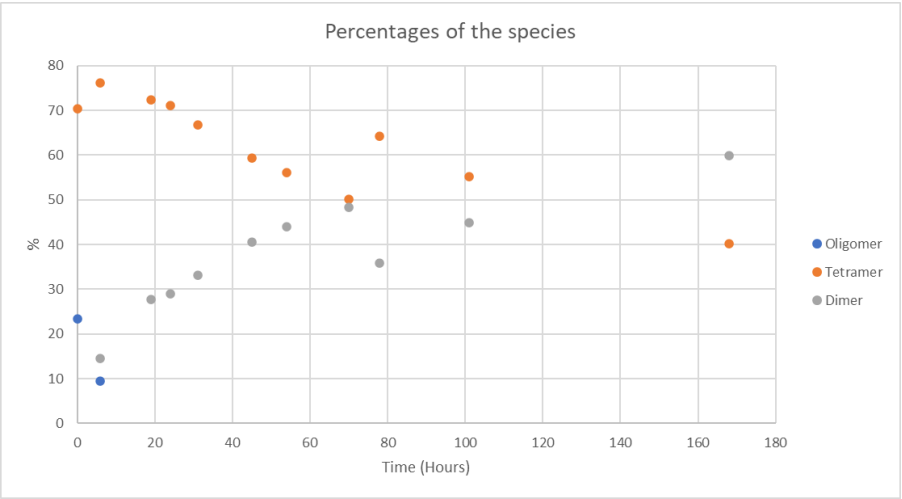

Figure 5 -- Percentage of subspecies present in the sample after incubation.

After performing the Size-Exclusion Chromatography, the changes in the abundance of different subspecies with time were observed. Figure 5 represents the relative changes of α-syn species in solution in time. At early stages of the incubation, a single peak, at the retention time (Rt) of 44 mins, fused with a smaller peak, at the Rt of 40 minutes (oligomer), and another peak, at Rt of 51 mins, can be observed. The Rt44 peak represents the tetramer. After 70 hours of incubation (T70), a mixture of two peaks can be observed. These peaks represent the tetramer and dimer. After 168 hours of incubation (T168), the sample show an equilibrium between the two species. Figure 5 represents the percentages of the different subspecies in each time of incubation. It is observable the confluence of the tetramer and dimer species into an equilibrium, reaching a nearly 50-50 split at T70. The T78 results, reveal an increase in the percentage of the tetramer and a decrease in the percentage of the dimer, while the T101 bring the values of the percentages closer again. In the T168, the percentage of the dimer was superior to the percentage of the tetramer. This might suggest that, after incubation, these subspecies converge into an equilibrium.

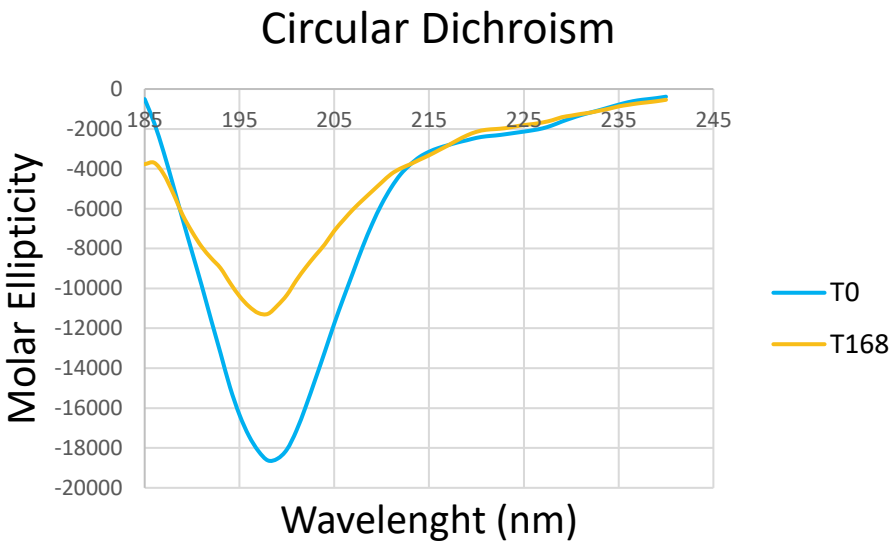

Figure 6 - Graphic Representation of the Circular Dichroism Assay in the wavelength range comprised between 185nm and 240nm for the T0 and T168 samples of the control set.

In the circular dichroism assay, it was observed a decrease in the molar ellipticity value (Figure 6) in the T168 sample compared to the T0 sample in the random coil area (around 200 nm). However, when we analyse the percentage of conformations (Figure 7), it is observable that, not only a decrease in the random coil happened (78% in T0 to 67% in T168), but also an increase of 8% in the strands and of 4% in the turns (11%, in T0, and 19%, in T168, Strands and 8%, in T0, and 12%, in T168, Turns). The α-helix percentage

didn't reveal any change, with 3% in all samples. Overall, the structural data suggests a gain of regular secondary structure with time.

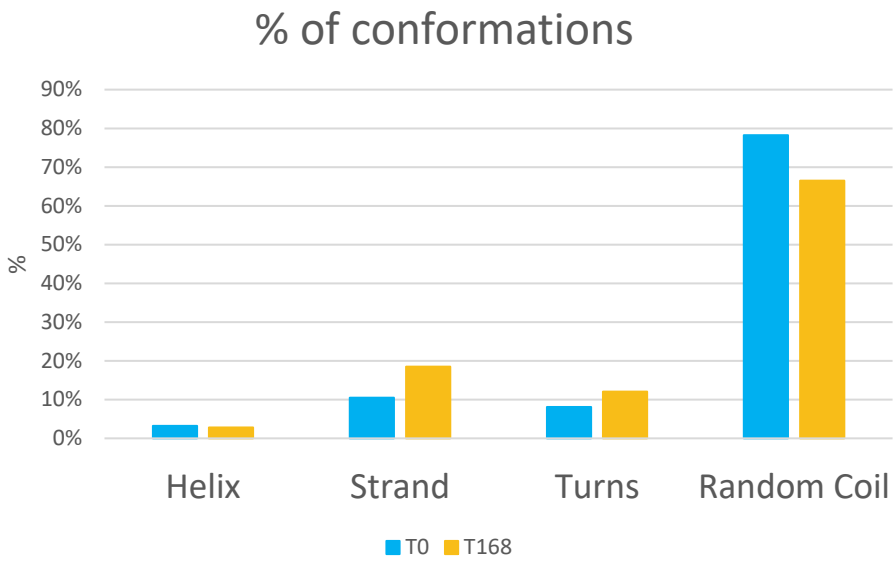

Figure 7 - Graphic representation of the percentage of conformations through the circular dichroism assay, obtained by analysis in the DichroWeb Website.

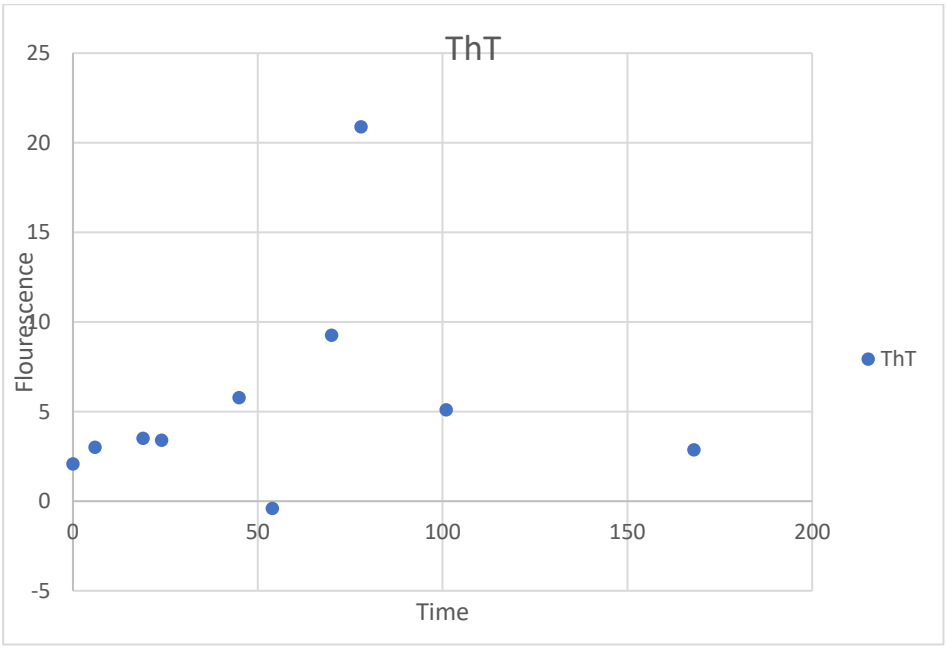

Figure 8 - Graphic representation of the values for the ThT assay at 482 nm.

The results of the fluorescence assay (Figure 8) do not reveal any tendency or significant variation in the signal able to lead to a conclusion in whether there is fibril formation or not.

3.2 Behaviour of α-syn in solution at different concentrations

Two assays were carried out at different concentrations in order to analyse the behaviour of the protein at above mentioned concentrations. The concentrations used were 0,66mg/ml for the first assay and 0,18mg/ml for the second assay.

Figure 9 represents the chromatograms for the time 0 at both assays in order to establish a comparison between them. As stated before, in the first assay, the dominant species was the tetrameric structure, with the presence of oligomers and a smaller presence of the dimeric structure. In the second assay, it is observable the presence of tetramers in the tallest point of the mixed peak, around the 43-minute mark, followed by dimeric structures, around the 48-minute mark. The other alterations in the baseline are due to the apparatus limitation since low concentration of protein is being applied. Thus, any variations in the electrical signal from the equipment may lead to baseline changes.

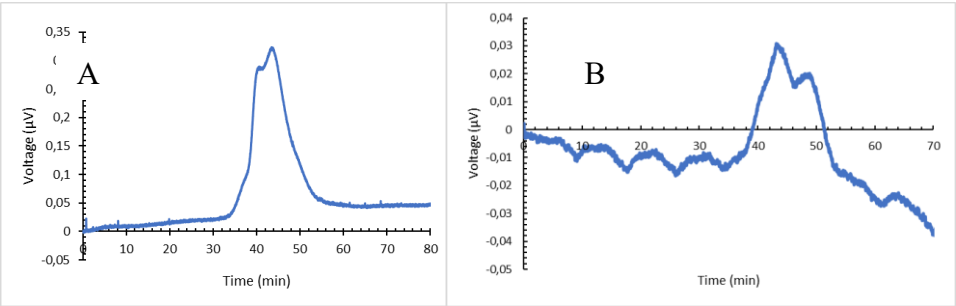

Figure 9 - Comparison between T0 on the samples of **(A)** 0,66mg/ml and **(B)** 0,18mg/ml of α-syn.

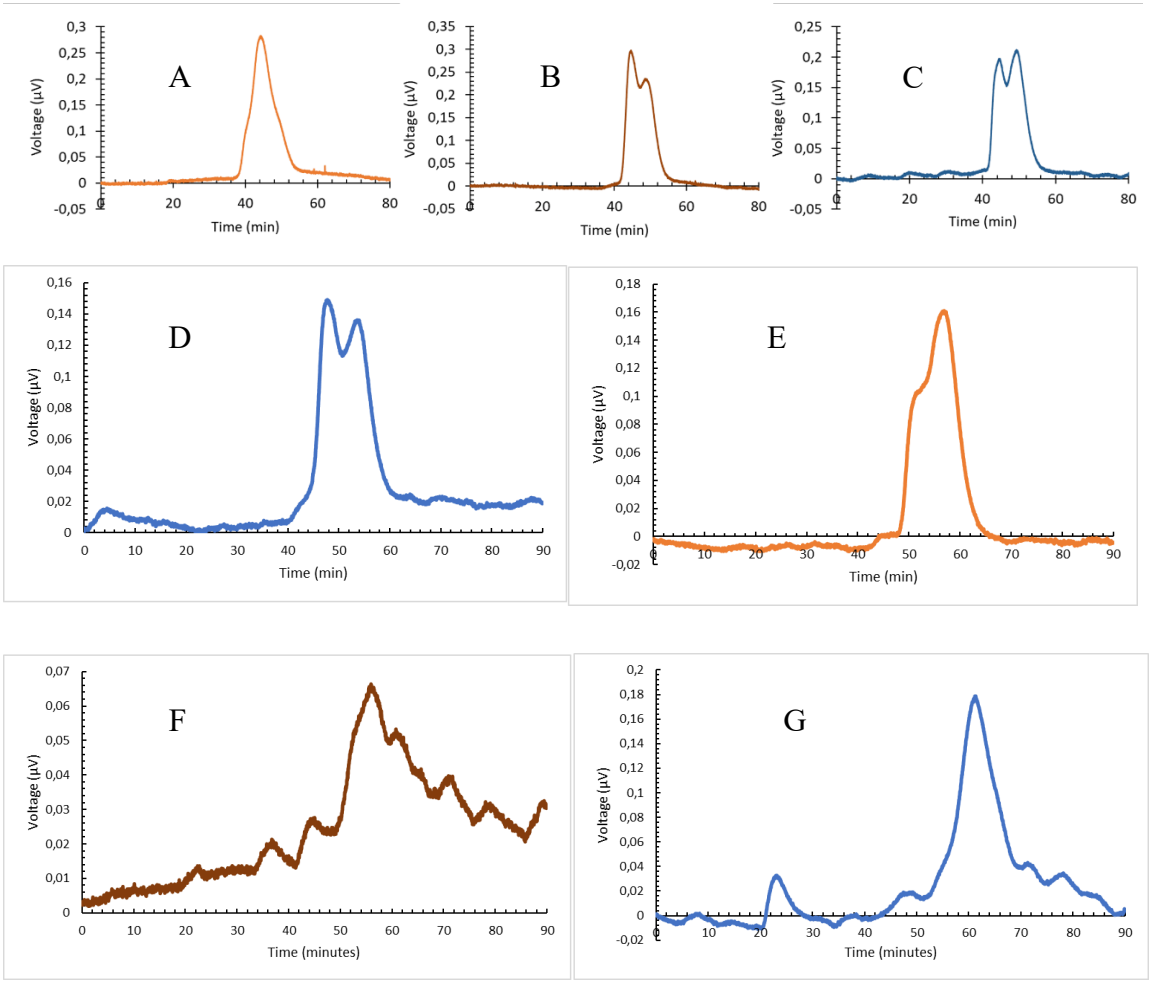

Figure 10- Comparison between the chromatograms of subspecies present in the samples from assay 1 and assay 2, at **(A)** 6 hours, 0,66mg/ml **(B)** 70 hours, 0,66mg/ml **(C)** 168 hours, 0,66mg/ml, **(D)** 24 hours, 0,18mg/ml, **(E)** 46 hours, 0,18mg/ml, **(F)** 92 hours, 0,18mg/ml and **(G)** 186 hours, 0,18mg/ml.

The comparison of these results (Figure 10) indicates that, although there is an equilibrium between two major species tetramer and dimer, towards the later stages of assay 1, in assay 2 that dynamic equilibrium never happens. Even though there is an apparent equilibrium in Figure 10D, that equilibrium is between dimeric and monomeric structures contrarily to the equilibrium between tetrameric and dimeric structures in Figure 10C. In Figure 10E, there is a small variation in the baseline at the 47-minute mark indicating the presence of dimeric structures, followed by a mixed peak of at the 53 and 57-minute marks. These peaks represent a monomeric structure (53 minutes) and a modified monomeric structure (57 minutes) which is probably more compact and or a molten globule (Judy & Kishore, 2019) interacting with the column matrix. In Figure 10F, there are two small peaks at the 36 and 44-minute mark representing molecules of

higher molecular weight which indicates the aggregation of monomeric and/or modified monomeric structures. The larger peak that follows has a small variation in the 53-minute mark representing the monomeric structure and the larger peak at 57-minute mark representing the modified monomeric species. In Figure 10G, there is a small peak at the 49-minute mark representing the dimeric structure, a variation in the profile of the larger peak at the 55-minute mark, representing the monomeric structure and the larger peak representing the modified monomeric structures.

Figure 11 represents the percentages of the different species. Unlike in assay 1 (Figure 11A), where there is a clear tendency to the dynamic equilibrium between dimer and monomer, in assay 2 (Figure 11B), there is no visible equilibrium, but a tendency of evolution towards a modified and more compact type of monomer. At 0 hours, the sample showed to be mostly tetrameric, with a considerable percentage of dimer and a small percentage of monomer, however, after 24 hours, the percentage of dimer increased slightly, while the percentages of tetramer and monomer inverted, suggesting a migration towards that structural form. After 46 hours, the percentage of dimeric structures was almost 0, and the monomeric percentage also decreased to nearly half of what it was 22 hours earlier. However, it is observable that there was a new structural type with the highest percentage in this time stamp, the modified and more compact monomer. The time stamps after 46 hours were not included in the graphic due to the several variations in the chromatogram, directly caused by the several peaks that appeared after the 60-minute mark in the SECs, revealing an abundance of molecules with lower molecular weight than the monomer. Table 1 and Table 2 show the percentage values for the different species. In some situations, the percentages do not add up to 100% due to some intermediate species that were purposefully left out in order to facilitate comprehension.

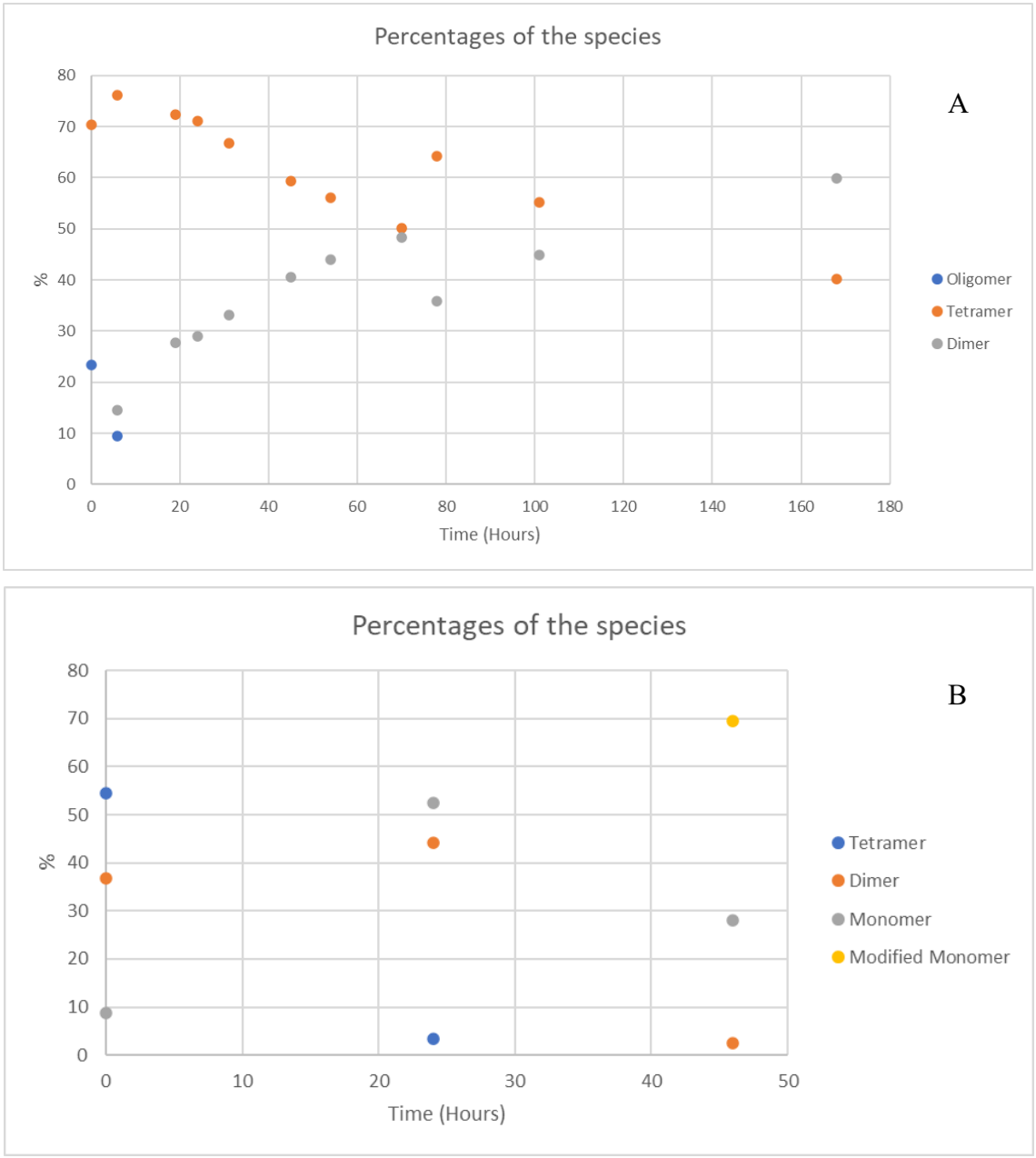

Figure 11 – Comparison of the percentage of subspecies present in the samples after incubation. **(A)** Represents the percentages of species in the sample from assay 1 and **(B)** represents the species from assay 2.

Table 1 - Percentages of species in the sample at higher α-syn concentration

	0 Hours	6 Hours	19 Hours	24 Hours	31 Hours	45 Hours	54 Hours	70 Hours	78 Hours	101 Hours	168 Hours
Oligomer	6.3%	9.4%									
Tetramer	23.3%	76.1%	72.3%	71.1%	66.8%	59.4%	56.1%	50.1%	64.2%	55.1%	40.1%
Dimer	70.4%	14.6%	27.7%	28.9%	33.2%	40.6%	43.9%	48.4%	35.8%	44.9%	59.9%

Table 2 - Percentages of species in the sample at lower protein concentration

	0 Hours	24 Hours	46 Hours
Oligomer	9%		
Tetramer	9.3%		
Dimer	47.8%	3%	2.6%
Monomer	15.7%	15.7%	28%
Modified Monomer		49%	69.4%

3.3 Influence of CBD in α-syn

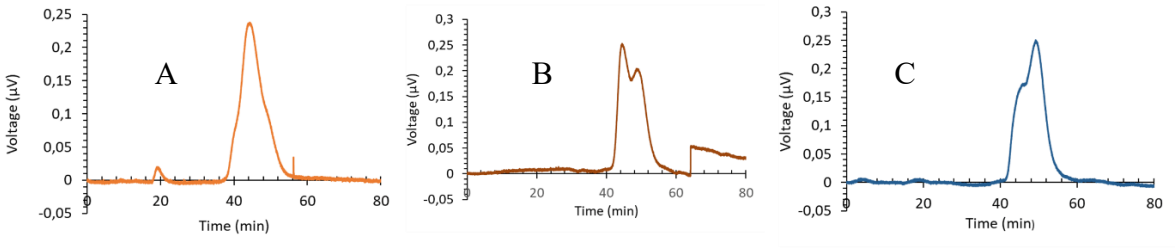

Figure 12 - Changes in the subspecies present in the samples with CBD at **(A)** 6 hours **(B)** 70 hours and **(C)** 168 hours. The results from the size-exclusion chromatography revealed an equilibrium between the tetramer and the dimer species, however, opposite to what happened in the control sample, the T168 sample with CBD revealed an increase in the percentage of dimer.

Similar to what happed in the early stages of the incubation in the control sample, a single peak, at the Rt of 44 mins, fused with a smaller peak, Rt of 40 minutes (oligomer), as well as another small peak, at the Rt of 51 mins, was observed, representing the tetramer (Rt44) and the dimer (Rt50). After 70 hours of incubation (T70), a mixture of two peaks can also be observed, only this time the difference between the tetramer and the dimer relative amount is slightly more pronounced. Nevertheless, after 168 hours of incubation (T168), the sample shows an increase in the dimer, differing from the control sample. The results suggest that CBD change the equilibrium between the tetramer and the dimer to the dimer

Regarding the percentages of the different subspecies in the sample in the presence of CBD (Figure 13), the similar percentage of tetramer and dimer at the T70 can be observed. At T78, like in the control sample, the tetramer has a higher percentage than the dimer. Nonetheless, in the CBD sample at the T101 the dimer already has a higher percentage than the tetramer, leading to an even greater gap at T168. These results might indicate that the CBD tend to help stabilizing the dimer in detriment of the equilibrium observed in the control sample.

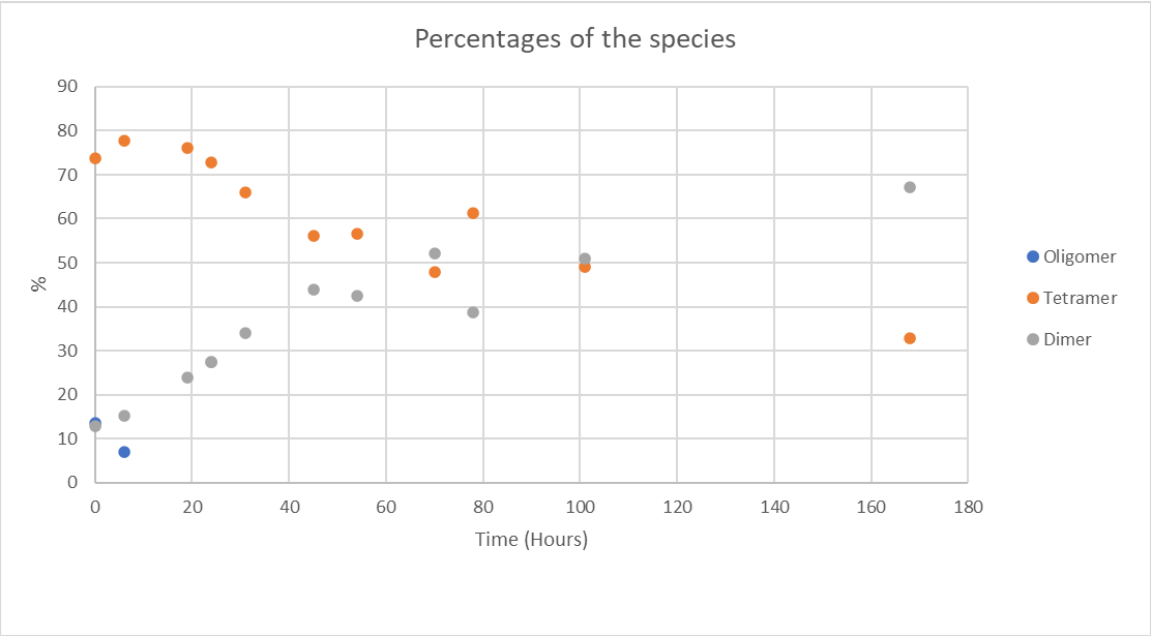

Figure 13 - Percentage of subspecies present in the sample with CBD after incubation

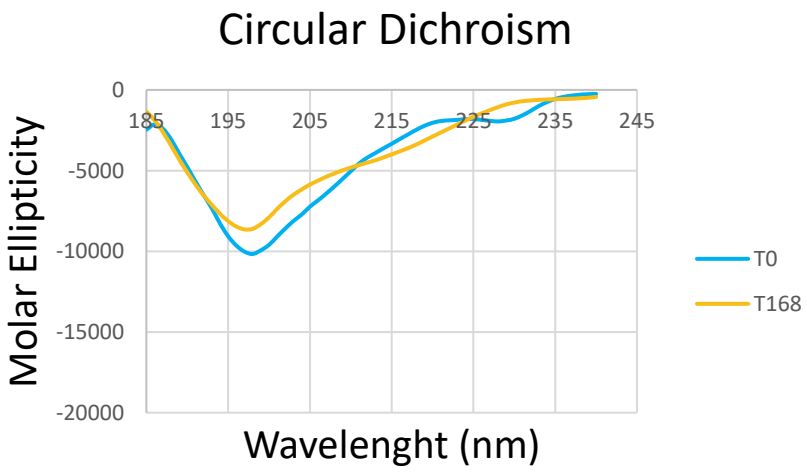

Figure 14 - Graphic Representation of the Circular Dichroism Assay in the wavelength range comprised between 185nm and 240nm for the T0 and T168 samples with CBD.

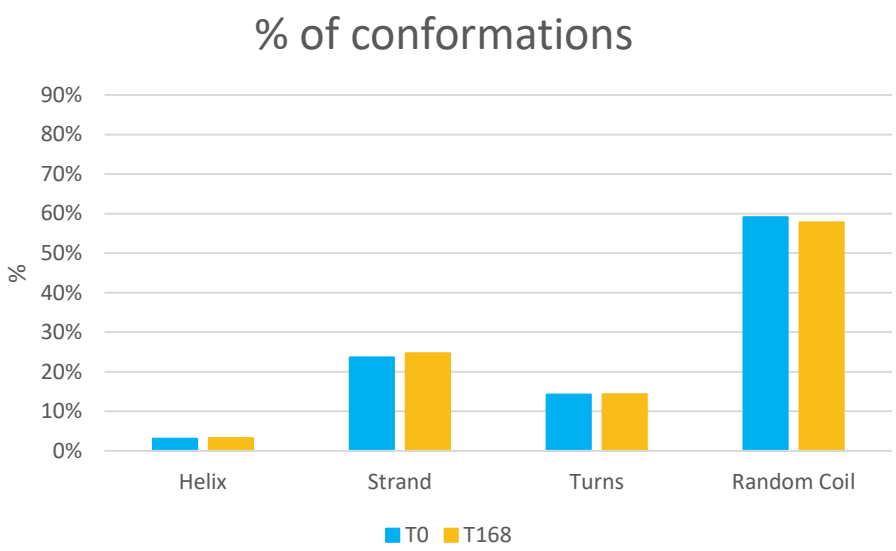

Figure 15 - Graphic representation of the percentage of conformations in the CBD sample through the circular dichroism assay, obtained by analysis in the DichroWeb Website

Figure 14 shows that the variation between the T0 and T168 Molar Ellipticity is not as pronounced as in the control sample in the random coil area (around 200nm). Furthermore, the variation of the percentages between the secondary structures' conformations in the presence of CBD (Figure 15), is almost inexistant, with 3% in both samples for the Helix conformation, and 14% for the Turns conformation in both samples. The Strand conformation had a 1% increase (24% in T0 and 25% in T168) and the Random Coil conformation had a 1% decrease (59% in the T0 sample and 58% in the T168 sample). However, comparing the results from the control sample and sample in presence of CBD, it is noticeable that the percentages of the conformations in the CBD sample at T0 are quite similar to the percentages of the conformations in the control sample at T168 (Table 3), suggesting that CBD decrease the amount of Random Coil conformation.

Table 3 – Comparison of the percentages of conformations in the control sample T168 and the CBD sample at T0

	Helix	Strands	Turns	Random Coil
Control T168	3%	12%	19%	67%
CBD T0	3%	14%	24%	59%

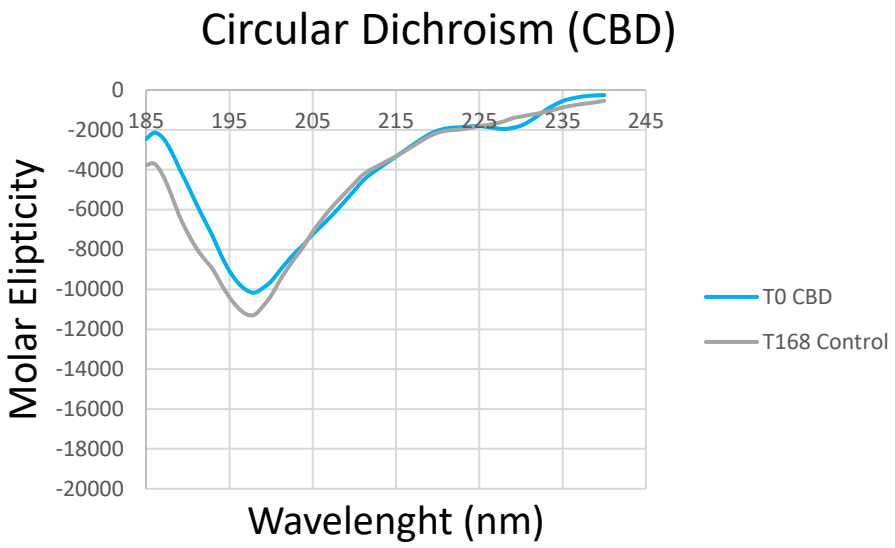

Figure 16 – Comparison of the graphic representations of the T0 CBD sample and the T168 control sample

The results from this assay suggest that the presence of CBD in the sample might have had an immediate impact in the alteration of the secondary structure of the protein.

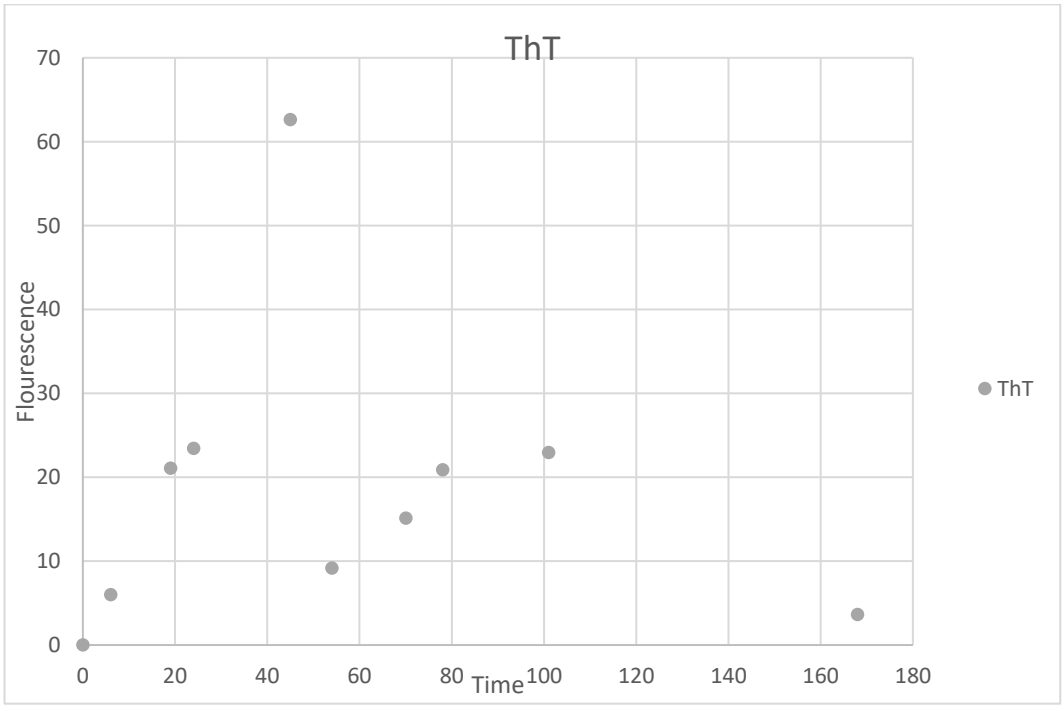

Figure 17 - Graphic representation of the values for the ThT assay at 482 nm for the CBD sample.

In similarity to the control sample, in the ThT assay, no conclusions can be drawn, as there is no clear tendency or significant variation to assess the presence of fibers in the samples.

3.4 Influence of CBD in α-syn at different concentrations

Figure 18 represents the chromatograms for the time 0 at both assays with CBD in order to establish a comparison between them. Just like the control sample in the first assay (Figure 18A), the dominant species was the tetrameric structure, with the presence of oligomers and a smaller presence of the dimeric structure. In the second assay (Figure 18B), it is observable the presence of tetramers and oligomers in the beginning of the slope towards the peak, in the time stamps comprised between 38 and 45 minutes. However, in the tallest point of the mixed peak, around the 49-minute mark, dimeric structures, around the 48-minute mark are the dominant structure in this chromatogram. A small presence of monomers, around the 54-minute mark can also be observed. The other alterations in the baseline could be already the modified monomeric structure forming.

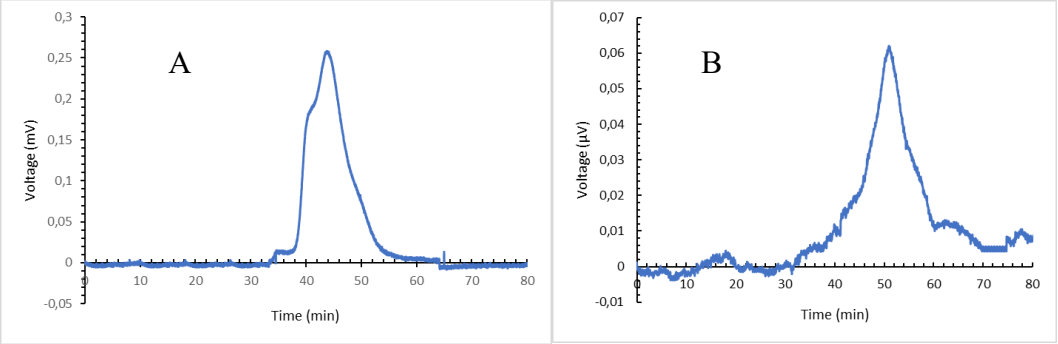

Figure 18 – Comparison between T0 on the samples of **(A)** 0,66mg/ml of α-syn with 1,5724mg/ml CBD and **(B)** 0,18mg/ml of α-syn with 0,4289mg/ml CBD

The comparison of these results (Figure 19) indicates that, although there is an equilibrium between two major species tetramer and dimer, towards the later stages of assay 1, in assay 2 that dynamic equilibrium never happens. That also happened in the control samples for the assay with lower concentration of α-syn. Just like in the control samples, there is an equilibrium in Figure 19D between dimeric and monomeric structures contrarily to the equilibrium between tetrameric and dimeric structures in Figure 19B and 19C, with the later having a tendency towards the dimer. In Figure 19E, there is an

alteration of the peak, with the dimer at the 49-minute mark but the mixed peak this time being a mixture of monomeric (53 minutes) and modified monomeric (59 minutes) structures, revealing a tendency towards the modified monomeric structure. In Figure 19F, there is a small peak corresponding to the dimer at the 47-minute mark, as well as a small monomeric peak at the 53-minute mark. In this chromatogram, it is clear that the dominant species is the modified monomer. The tall peaks after the 60-minute mark represent the species of lower molecular weight. In Figure 19G, larger molecules can be observed, due to the aggregation of the modified monomeric species forming a larger oligomer.

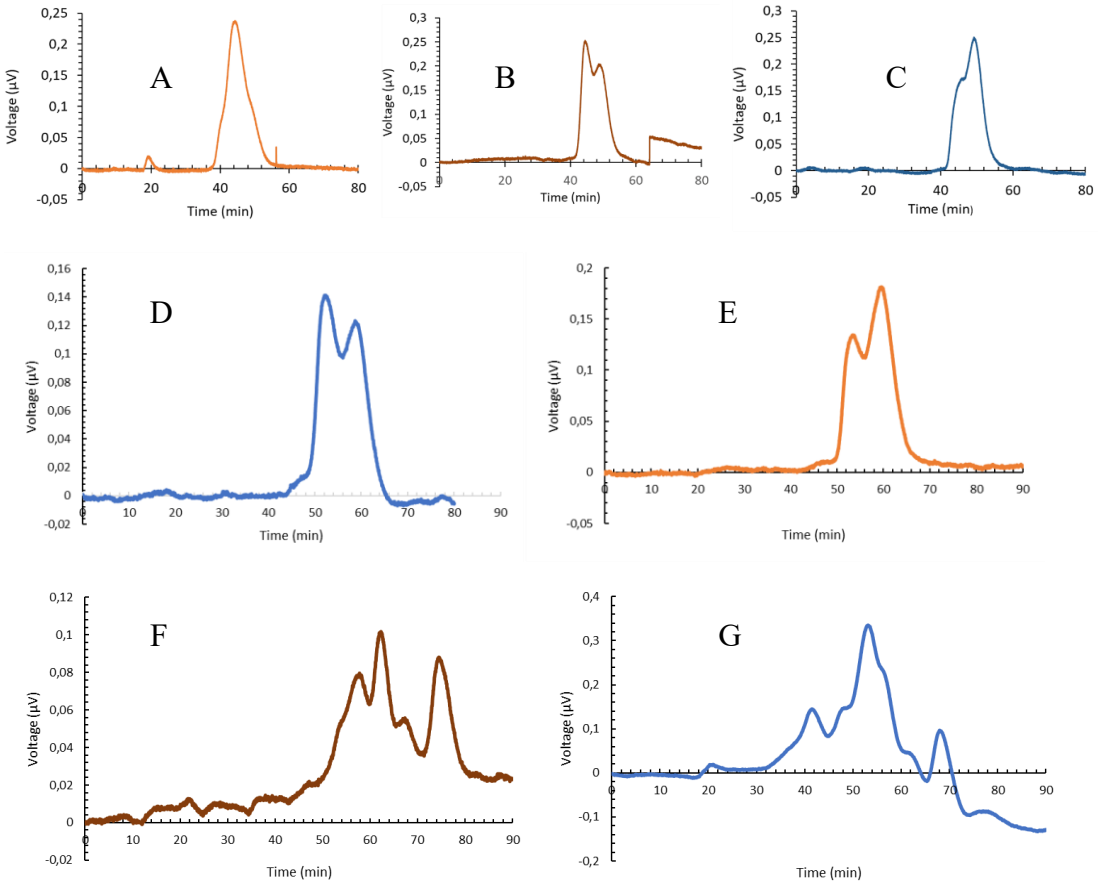

Figure 19 - Comparison between the subspecies present in the samples with CBD at **(A)** 6 hours, 0,66mg/ml of α-syn with 1,5724mg/ml CBD, **(B)** 70 hours, 0,66mg/ml of α-syn with 1,5724mg/ml CBD, **(C)** 168 hours 0,66mg/ml of α-syn with 1,5724mg/ml CBD, **(D)** 24 hours, 0,18mg/ml of α-syn with 0,4289mg/ml CBD **(E)** 46 hours, 0,18mg/ml of α-syn with 0,4289mg/ml CBD, **(F)** 92 hours, 0,18mg/ml of α-syn with 0,4289mg/ml CBD and **(G)** 186 hours, 0,18mg/ml of α-syn with 0,4289mg/ml CBD.

In Figure 20A comparison between the percentages of species in the samples with CBD was made in order to assess the changes over time. In Figure 16A we can observe the establishment of an equilibrium between tetramer and dimer after 72 hours of incubation, with an increase in the dimer in the later stages of the experiment. In Figure 20B, at 0 hours, there was a small percentage of oligomers and tetramers in the sample, with a percentage slightly higher of monomers and nearly 50% of dimers. After 24 hours of incubation, there was a decrease in the percentage of dimers in the sample, with monomers maintaining around the same values as in 0 hours and higher percentage of modified monomers, with nearly 50%. After 46 hours of incubation, the percentage of dimeric structures remained low, while the percentages of monomers and modified monomers increased. In some situations, the percentages do not add up to 100% due to some intermediate species that were purposefully left out in order to facilitate comprehension.

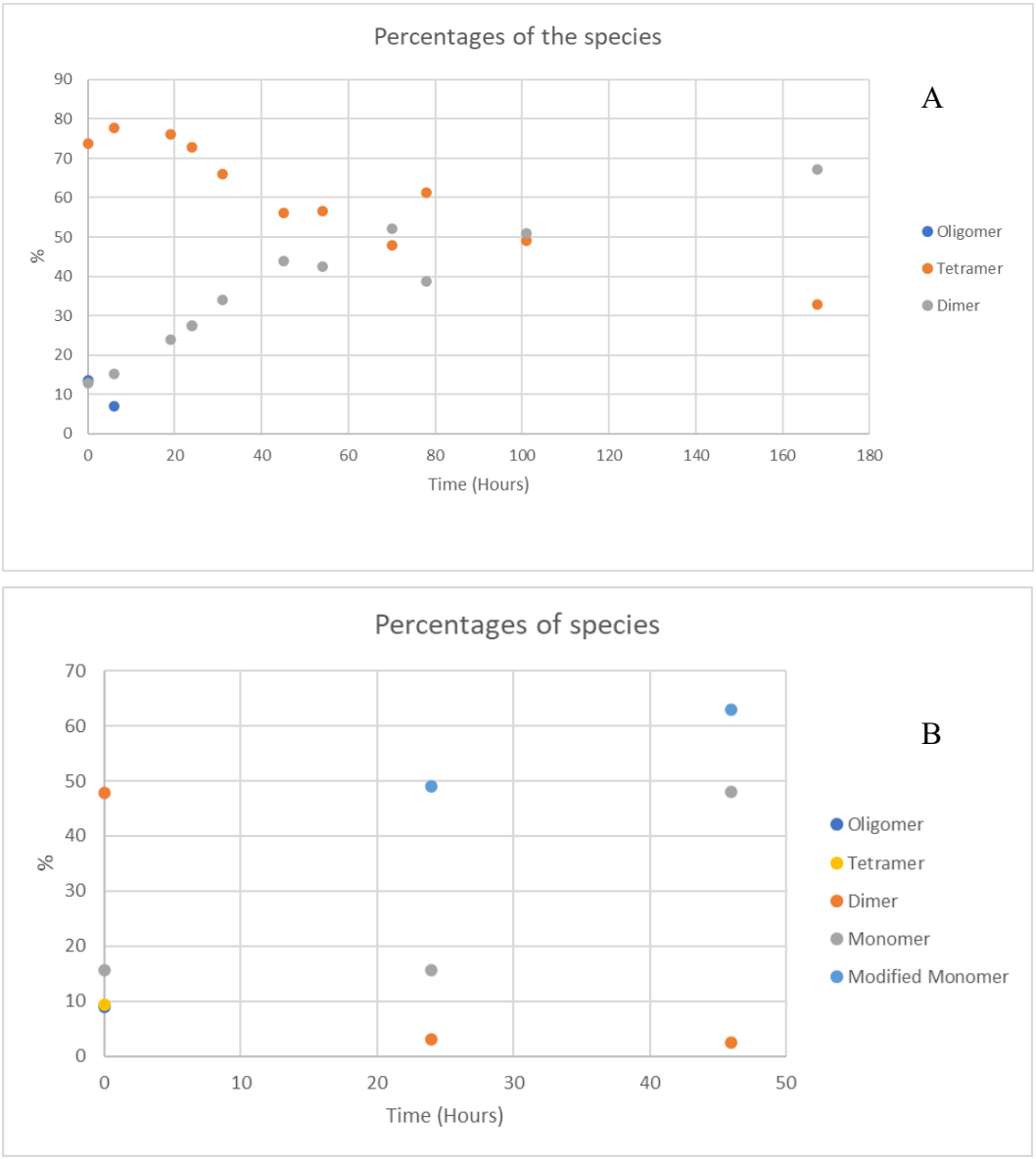

Figure 20 - Comparison of the percentage of subspecies present in the samples with CBD after incubation. **(A)** Represents the percentages of species in the sample from assay 1 (0,66mg/ml of α-syn with 1,5724mg/ml CBD) and **(B)** represents the species from assay 2 (0,18mg/ml of α-syn with 0,4289mg/ml CBD).

Table 4 - Percentages of the different species in the CBD samples of higher concentration.

	0 Hours	6 Hours	19 Hours	24 Hours	31 Hours	45 Hours	54 Hours	70 Hours	78 Hours	101 Hours	168 Hours
Oligomer	13.5%	7%									
Tetramer	73.7%	77.8%	76.2%	72.8%	65.9%	56.1%	56.6%	47.8%	61.2%	49%	32.9%
Dimer	12.8%	15.3%	23.8%	27.2%	34.1%	43.9%	42.5%	52.2%	38.8%	51%	67.1%

Table 5 - Percentages of the different species in the CBD sample of lower concentration.

	0 Hours	24 Hours	46 Hours
Oligomer	9%		
Tetramer	9.3%		
Dimer	47.8%	3%	2.4%
Monomer	15.7%	15.7%	34.7%
Modified Monomer		49%	62.9%

Table 4 and Table 5 show the percentage values for the different species.

3.5 Overview of the results and proposal of a model

According to our data, α-syn aggregation starts with the formation of modified monomers that emerge from the native monomer after dimer dissociation. To the best of our knowledge is the first time that the putative amyloid intermediate is describe as a modified α-syn monomer. Actually, Villar-Piqué *et al.* (2015), Mehra *et al.* (2019) and Lashuel *et al.* (2012), are elusive regarding the starting point of aggregation, mentioning the subsequent steps, where aggregation is the result from the build-up from oligomers into small fibrils and then larger fibrils, or the fragmentation of fibrils leading to a pool of steady state oligomers.

The results of the study of the behaviour of α-syn in solution revealed that there is a dynamic equilibrium between the tetrameric and dimeric structures in the higher concentration assay and the formation of aggregates of modified monomeric structure in the lower concentration assay. This leads to the conclusion that the concentration of the protein in solution plays a role in the aggregation.

Regarding the results from the assay with CBD, the results from the circular dichroism for the assay with the highest concentration showed that the percentages of the conformations in the beginning of the CBD sample were similar to the percentages at the end of the control sample. This may indicate that CBD play a role in the stabilisation of the conformational changes. In the SEC, for the assay with the highest concentration, an equilibrium was observed with a tendency towards the dimeric structure. In the assay with lower concentration, the results of the SEC showed a prevalence of the modified monomeric structure and the formation of aggregates of these modified structures. The suggested model consists of the interpretation of these results.

Overall, this work had as an objective to study the effects of phytocannabinoids in α-syn. The results obtained by this experiment suggests that there is an interaction between α-syn and cannabidiol, judging by the changes in dimer tetramer equilibrium and the changes in secondary structure motifs.

4 Conclusion

The present study aimed to study the impact of phytocannabinoids on α-syn aggregation, has produced four main observations:

1. Native α-syn exists in solution as an equilibrium between n-tetramer ↔ tetramer ↔ dimer ↔ monomer.
2. The previously mentioned equilibrium seems to shift left or right depending on the concentration.
3. The native monomer give rise to modified monomers.
4. Cannabidiol seems to stabilize the monomeric species

Based on the for above mentioned empirical observations, a model for α-syn is proposed to gather the data.

The proposed model of α-syn aggregation consists of an equilibrium between the tetrameric species with the dimeric species, as observed in assay 1. Furthermore, the dimeric species tend to evolve into a modified monomeric species of lower molecular weight, which forms aggregates creating high molecular weight aggregates.

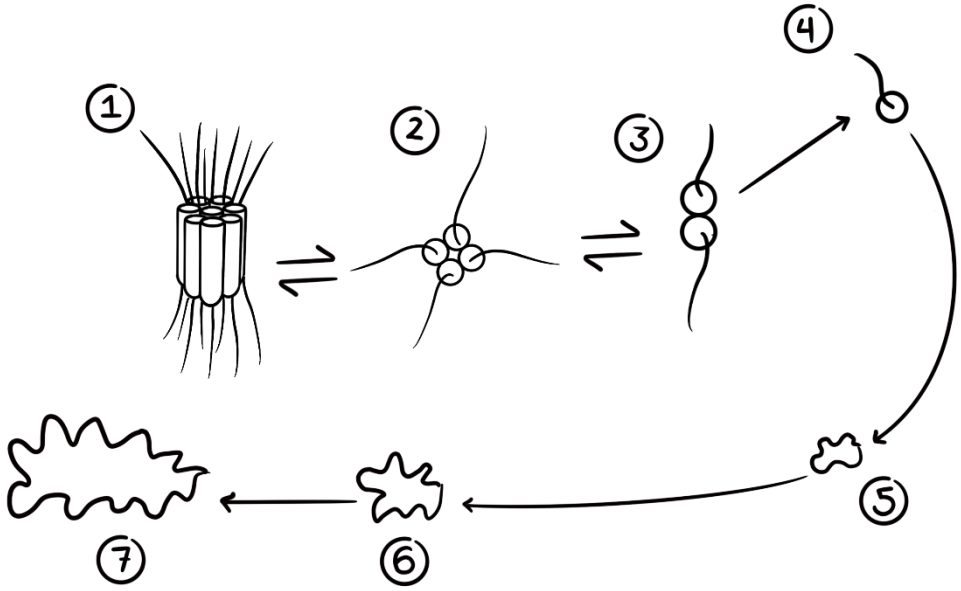

Figure 21 – Proposed molecular model for the aggregation of α-syn. **(1)** Oligomer, **(2)** Tetramer, **(3)** Dimer, **(4)** Monomer, **(5)** Modified Monomer, **(6)** Beginning of aggregation, **(7)** Aggregates with high molecular weight.

In Figure 21, the proposed model is presented. As observed in the assay 1, the presence of oligomers at the start of the experiment before incubation was noted, along with tetramers and dimers. Tetramers and dimers appeared to be in a dynamic equilibrium between them, depending on a-syn concentration, not changing further into other species, being them larger or smaller at moderated concentrations. In assay 2, the initial sample revealed the presence of tetramers, dimers, and monomers. During incubation, the dynamic equilibrium formed was between dimers and monomers, which then lead to a prevalence of a modified monomeric structure. As the experiment progressed, the modified monomeric structure started to aggregate with and by the end of the experiment, larger molecules had formed, leading to aggregates with high molecular weight.
For the assay with lower concentration, the ThT and CD tests were not performed due to the concentration being too low to be accurate.

Further studies should include a wider range of concentrations and the ThT and CD tests for all concentrations. Different phytocannabinoids should also be included, being them natural or synthetic, in order to understand how the different phytocannabinoids interact with α-syn.

References

Back, J. F., Oakenfull, D., & Smith, M. B. (1979). Increased thermal stability of proteins in the presence of sugars and polyols. *Biochemistry*, *18*(23), 5191–5196. https://doi.org/10.1021/bi00590a025

Braak, H., Bohl, J. R., Müller, C. M., Rüb, U., de Vos, R. A. I., & Del Tredici, K. (2006). Stanley Fahn lecture 2005: The staging procedure for the inclusion body pathology associated with sporadic parkinson's disease reconsidered. *Movement Disorders*, *21*(12), 2042–2051. https://doi.org/10.1002/mds.21065

Braak, H., Tredici, K. D., Rüb, U., de Vos, R. A. I., Jansen Steur, E. N. H., & Braak, E. (2003). Staging of brain pathology related to sporadic parkinson's disease. *Neurobiology of Aging*, *24*(2), 197–211. https://doi.org/10.1016/s0197-4580(02)00065-9

Burstein, S. (2015). Cannabidiol (CBD) and its analogs: A review of their effects on inflammation. *Bioorganic & Medicinal Chemistry*, *23*(7), 1377–1385. https://doi.org/10.1016/j.bmc.2015.01.059

Chen, J. Y., Parekh, M., Seliman, H., Bakshinskaya, D., Dai, W., Kwan, K., Chen, K. Y., & Liu, A. Y. C. (2018). Heat shock promotes inclusion body formation of mutant Huntingtin (mHtt) and alleviates MHTT-induced transcription factor dysfunction. *Journal of Biological Chemistry*, *293*(40), 15581–15593. https://doi.org/10.1074/jbc.ra118.002933

Cookson, M. (2009). α-Synuclein and neuronal cell death. Molecular Neurodegeneration, 4(1), 9. doi: 10.1186/1750-1326-4-9

Cooray, R., Gupta, V., & Suphioglu, C. (2020). Current aspects of the endocannabinoid system and targeted THC and CBD phytocannabinoids as potential therapeutics for parkinson's and alzheimer's diseases: A Review. *Molecular Neurobiology*, *57*(11), 4878–4890. https://doi.org/10.1007/s12035-020-02054-6

Dauer, W., & Przedborski, S. (2003). Parkinson's disease. *Neuron*, *39*(6), 889–909. https://doi.org/10.1016/s0896-6273(03)00568-3

Dimant, H., Ebrahimi-Fakhari, D., & McLean, P. J. (2012). Molecular chaperones and co-chaperones in parkinson disease. *The Neuroscientist*, *18*(6), 589–601. https://doi.org/10.1177/1073858412441372

Farnsworth, N. R. (1969). Pharmacognosy and chemistry of 'cannabis sativa'. *Journal of the American Pharmaceutical Association (1961)*, *9*(8), 410–440. https://doi.org/10.1016/s0003-0465(16)30933-8

Ferreira, C., Almeida, C., Tenreiro, S., & Quintas, A. (2020). Neuroprotection or Neurotoxicity of Illicit Drugs on Parkinson's 184 Disease. Life, 10(6), 86. doi: 10.3390/life10060086

Henle, K. J., Peck, J. W., & Higashikubo, R. (1983). *Cancer Research*, *43*(4), 1624–1627.

Horton, R. H., Perry, M., Scrimgeour, G., & Moran, L. A. (2014). *Principles of biochemistry*. Pearson education.

Klucken, J., Shin, Y., Masliah, E., Hyman, B. T., & McLean, P. J. (2004). HSP70 reduces α-synuclein aggregation and toxicity. *Journal of Biological Chemistry*, *279*(24), 25497–25502. https://doi.org/10.1074/jbc.m400255200

Klucken, J., Outeiro, T. F., Nguyen, P., McLean, P. J., & Hyman, B. T. (2006). Detection of novel intracellular o-synuclein oligomeric species by fluorescence lifetime imaging. *The FASEB Journal*, *20*(12), 2050–2057. https://doi.org/10.1096/fj.05-5422com

Kriese, U., Schumann, E., Weber, W. E., Beyer, M., Brühl, L., & Matthäus, B. (2004). Oil content, tocopherol composition and fatty acid patterns of the seeds of 51 cannabis sativa L. genotypes. *Euphytica*, *137*(3), 339–351. https://doi.org/10.1023/b:euph.0000040473.23941.76

Judy, E., & Kishore, N. (2019). A look back at the molten globule state of proteins: Thermodynamic aspects. *Biophysical Reviews*, *11*(3), 365–375. https://doi.org/10.1007/s12551-019-00527-0

Lashuel, H. A., Overk, C. R., Oueslati, A., & Masliah, E. (2012). The many faces of α-synuclein: From structure and toxicity to therapeutic target. *Nature Reviews Neuroscience*, *14*(1), 38–48. https://doi.org/10.1038/nrn3406

Liang, J., Clark-Dixon, C., Wang, S., Flower, T. R., Williams-Hart, T., Zweig, R., Robinson, L. C., Tatchell, K., & Witt, S. N. (2008). Novel suppressors of α-synuclein toxicity identified using yeast. *Human Molecular Genetics*, *17*(23), 3784–3795. https://doi.org/10.1093/hmg/ddn276

Lin, P.-S., Kwock, L., & Hefter, K. (1981). Protection of heat induced cytoxicity by glycerol. *Journal of Cellular Physiology*, *108*(3), 439–443. https://doi.org/10.1002/jcp.1041080318

Mahoney-Sánchez, L., Bouchaoui, H., Ayton, S., Devos, D., Duce, J. A., & Devedjian, J.-C. (2021). Ferroptosis and its potential role in the physiopathology of parkinson's disease. *Progress in Neurobiology*, *196*, 101890. https://doi.org/10.1016/j.pneurobio.2020.101890

Mehra, S., Sahay, S., & Maji, S. K. (2019). A-synuclein misfolding and aggregation: Implications in parkinson's disease pathogenesis. *Biochimica Et Biophysica Acta (BBA) - Proteins and Proteomics*, *1867*(10), 890–908. https://doi.org/10.1016/j.bbapap.2019.03.001

Miles, A., Ramalli, S., & Wallace, B. (2021). <scp>DichroWeb</scp>, a website for calculating protein secondary structure from circular dichroism spectroscopic data. Protein Science, 31(1), 37-46. doi: 10.1002/pro.415

Ohgita, T., Namba, N., Kono, H., Shimanouchi, T., & Saito, H. (2022). Mechanisms of enhanced aggregation and fibril formation of parkinson's disease-related variants of α-synuclein. *Scientific Reports*, *12*(1). https://doi.org/10.1038/s41598-022-10789-6

Pertwee, R. G. (2009). The diverse CB1 and CB2receptor pharmacology of three plant cannabinoids: Δ9-tetrahydrocannabinol, cannabidiol and Δ9-tetrahydrocannabivarin. *British Journal of Pharmacology*, *153*(2), 199–215. https://doi.org/10.1038/sj.bjp.0707442

Pertwee, R. G. (2014). *Handbook of cannabis: Edited by Roger G. Pertwee*. Oxford University Press.

Polymeropoulos, M. H., Lavedan, C., Leroy, E., Ide, S. E., Dehejia, A., Dutra, A., Pike, B., Root, H., Rubenstein, J., Boyer, R., Stenroos, E. S., Chandrasekharappa, S., Athanassiadou, A., Papapetropoulos, T., Johnson, W. G., Lazzarini, A. M., Duvoisin, R. C., Di Iorio, G., Golbe, L. I., & Nussbaum, R. L. (1997). Mutation in the α-synuclein gene identified in families with parkinson's disease. *Science*, *276*(5321), 2045–2047. https://doi.org/10.1126/science.276.5321.2045

Pujols, J., Peña-Díaz, S., Pallarès, I., & Ventura, S. (2020). Chemical Chaperones as novel drugs for parkinson's disease. *Trends in Molecular Medicine*, *26*(4), 408–421. https://doi.org/10.1016/j.molmed.2020.01.005

Rubenstein, R. C., & Zeitlin, P. L. (2000). Sodium 4-phenylbutyrate downregulates HSC70: Implications for intracellular trafficking of ΔF508-CFTR. *American Journal of Physiology-Cell Physiology*, *278*(2). https://doi.org/10.1152/ajpcell.2000.278.2.c259

Shahmoradian, S. H., Lewis, A. J., Genoud, C., Hench, J., Moors, T. E., Navarro, P. P., Castaño-Díez, D., Schweighauser, G., Graff-Meyer, A., Goldie, K. N., Sütterlin, R., Huisman, E., Ingrassia, A., Gier, Y. de, Rozemuller, A. J., Wang, J., Paepe, A. D., Erny, J., Staempfli, A., … Lauer, M. E. (2019). Lewy pathology in parkinson's disease consists of crowded organelles and lipid membranes. *Nature Neuroscience*, *22*(7), 1099–1109. https://doi.org/10.1038/s41593-019-0423-2

Sreerama, N., & Woody, R. (2000). Estimation of Protein Secondary Structure from Circular Dichroism Spectra: Comparison of CONTIN, SELCON, and CDSSTR Methods with an Expanded Reference Set. Analytical Biochemistry, 287(2), 252-260. doi: 10.1006/abio.2000.4880

St Martin, J. L., Klucken, J., Outeiro, T. F., Nguyen, P., Keller-McGandy, C., Cantuti-Castelvetri, I., Grammatopoulos, T. N., Standaert, D. G., Hyman, B. T., & McLean, P. J. (2007). Dopaminergic neuron loss and up-regulation of chaperone protein mrna induced by targeted over-expression of alpha-synuclein in mouse substantia nigra. *Journal of Neurochemistry*. https://doi.org/10.1111/j.1471-4159.2006.04310.x

Thomas, B. F., & ElSohly, M. A. (2016). *The Analytical Chemistry of Cannabis: Quality Assessment, assurance, and regulation of medicinal marijuana and cannabinoid preparations*. Elsevier/RTI International.

Turner, S. E., Williams, C. M., Iversen, L., & Whalley, B. J. (2017). Molecular pharmacology of phytocannabinoids. *Progress in the Chemistry of Organic Natural Products*, 61–101. https://doi.org/10.1007/978-3-319-45541-9_3

van Stokkum, I., Spoelder, H., Bloemendal, M., van Grondelle, R., & Groen, F. (1990). Estimation of protein secondary structure and error analysis from circular dichroism spectra. Analytical Biochemistry, 191(1), 110-118. doi: 10.1016/0003-2697(90)90396-q

Villar-Piqué, A., Lopes da Fonseca, T., & Outeiro, T. F. (2015). Structure, function, and toxicity of alpha-synuclein: The Bermuda Triangle in Synucleinopathies. *Journal of Neurochemistry*, *139*, 240–255. https://doi.org/10.1111/jnc.13249

Wakabayashi, K., Tanji, K., Odagiri, S., Miki, Y., Mori, F., & Takahashi, H. (2012). The lewy body in parkinson's disease and related neurodegenerative disorders. *Molecular Neurobiology*, *47*(2), 495–508. https://doi.org/10.1007/s12035-012-8280-y

Wegrzynowicz, M., Bar-On, D., Calo', L., Anichtchik, O., Iovino, M., & Xia, J. *et al.* (2019). Depopulation of dense α-synuclein aggregates is associated with rescue of dopamine neuron dysfunction and death in a new Parkinson's disease model. Acta Neuropathologica, 138(4), 575- 595. doi: 10.1007/s00401-019-02023-x.

Yasuda, T., Nakata, Y., & Mochizuki, H. (2012). α-Synuclein and Neuronal Cell Death. Molecular Neurobiology, 47(2), 466-483. doi: 10.1007/s12035-012-8327-0

Appendix

Chromatograms from the SEC performed in the samples with higher concentration of α-syn in the presence of CBD from 0 hours (T0) until 215 hours (T215).

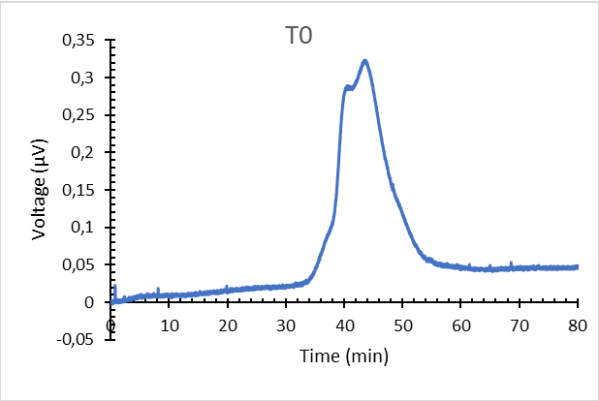

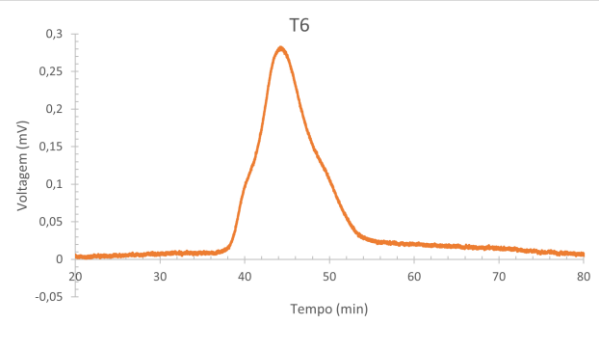

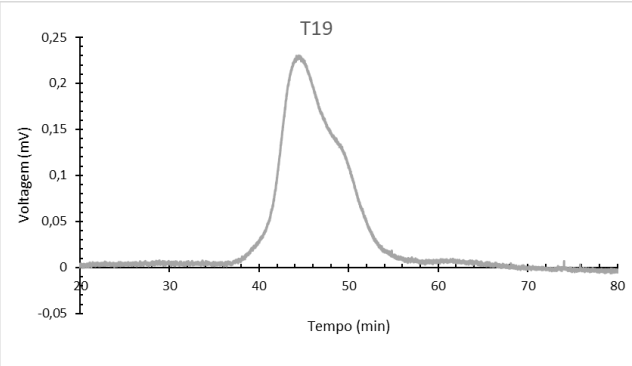

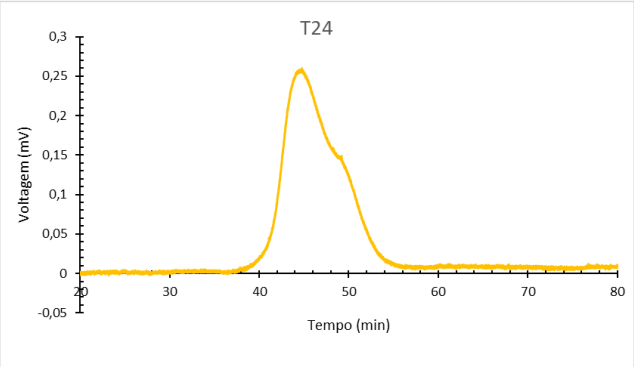

Appendix

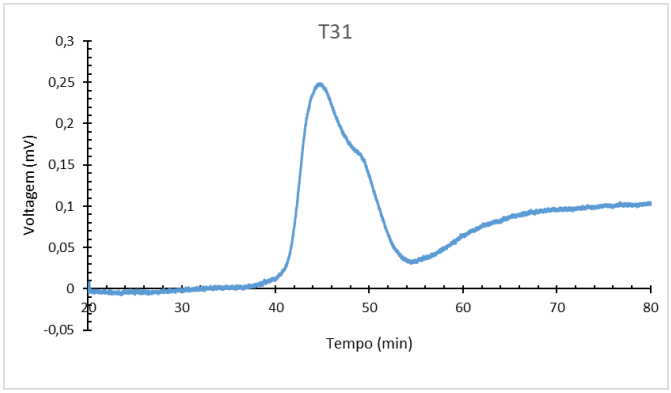
T31
Voltagem (mV)
Tempo (min)

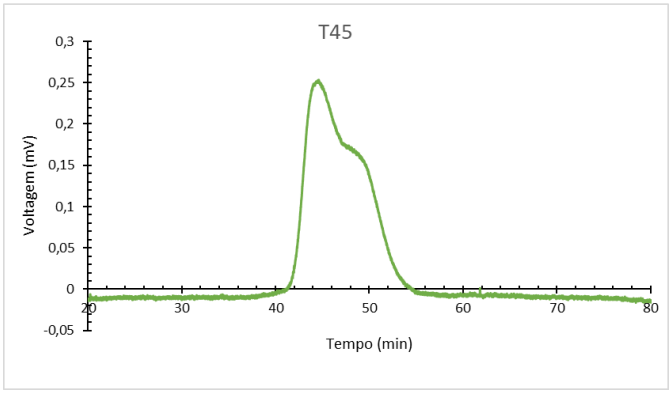
T45
Voltagem (mV)
Tempo (min)

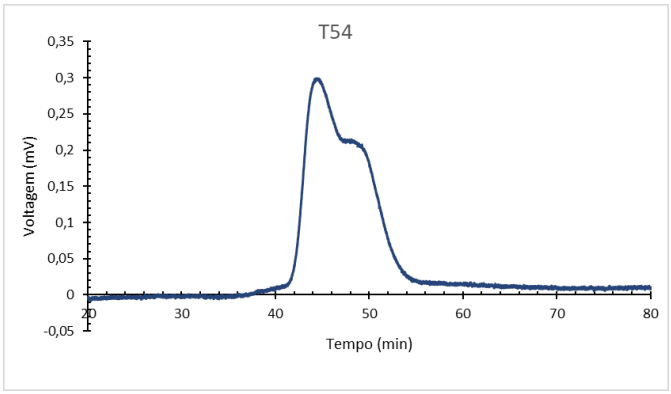
T54
Voltagem (mV)
Tempo (min)

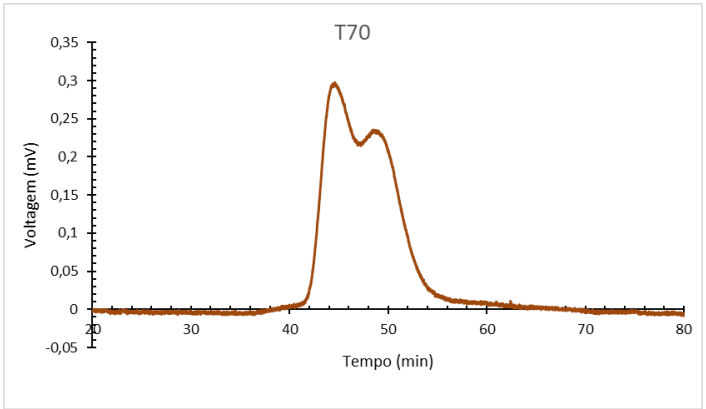
T70
Voltagem (mV)
Tempo (min)

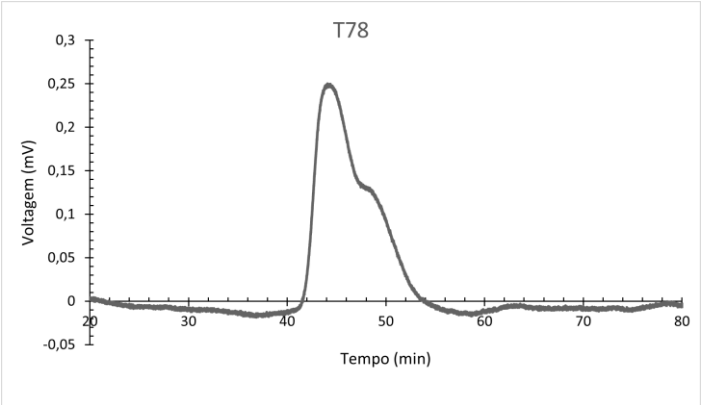
T78
Voltagem (mV)
0,3
0,25
0,2
0,15
0,1
0,05
0
-0,05
20
30
40
50
60
70
80
Tempo (min)

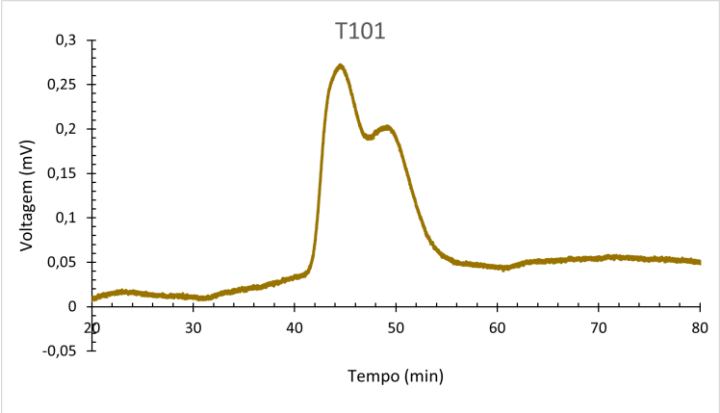
T101
Voltagem (mV)
0,3
0,25
0,2
0,15
0,1
0,05
0
-0,05
20
30
40
50
60
70
80
Tempo (min)

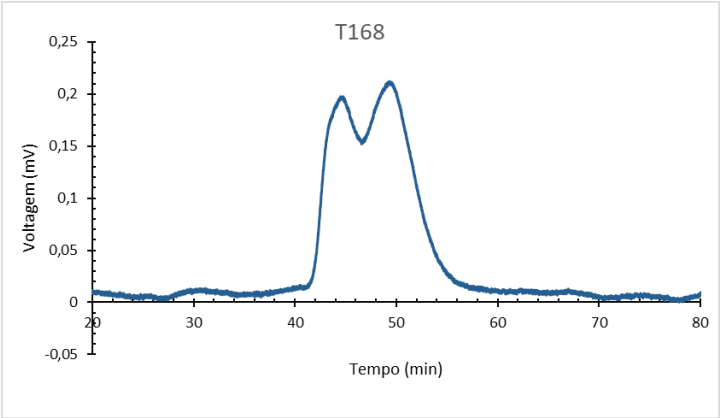
T168
Voltagem (mV)
0,25
0,2
0,15
0,1
0,05
0
-0,05
20
30
40
50
60
70
80
Tempo (min)

Appendix

Chromatograms from the SEC performed in the samples with higher concentration of α-syn in the presence of CBD from 0 hours (T0) until 215 hours (T215).

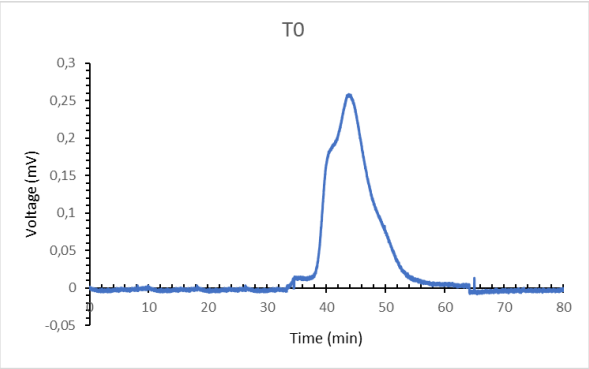

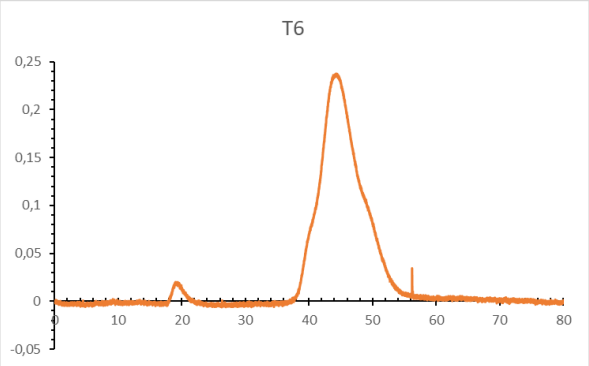

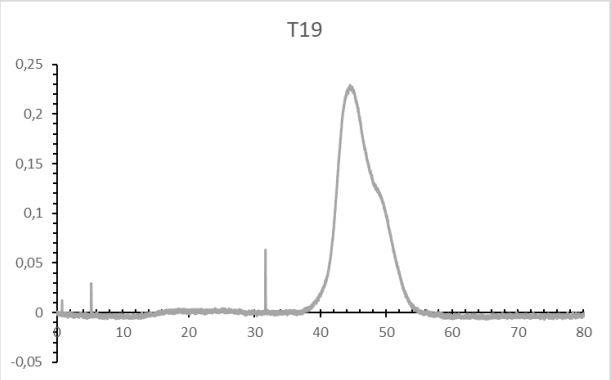

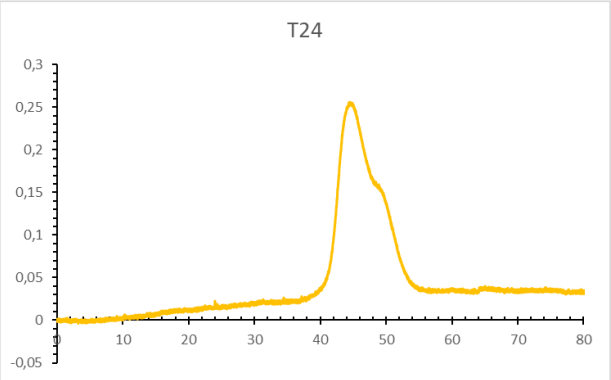

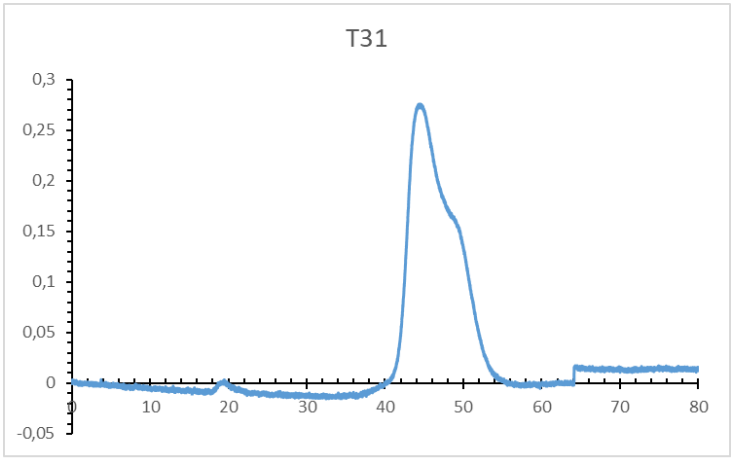
T31
0,3
0,25
0,2
0,15
0,1
0,05
0
-0,05
0
10
20
30
40
50
60
70
80

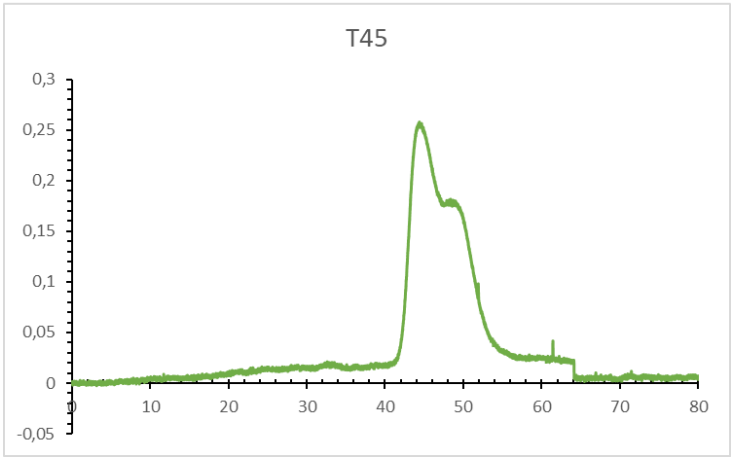
T45
0,3
0,25
0,2
0,15
0,1
0,05
0
-0,05
0
10
20
30
40
50
60
70
80

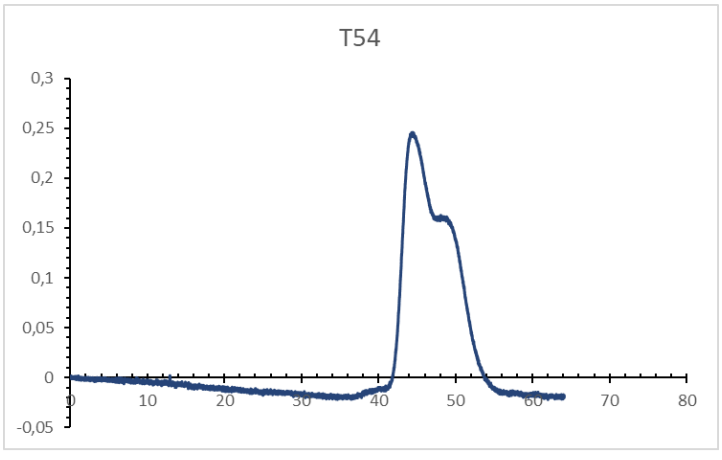
T54
0,3
0,25
0,2
0,15
0,1
0,05
0
-0,05
0
10
20
30
40
50
60
70
80

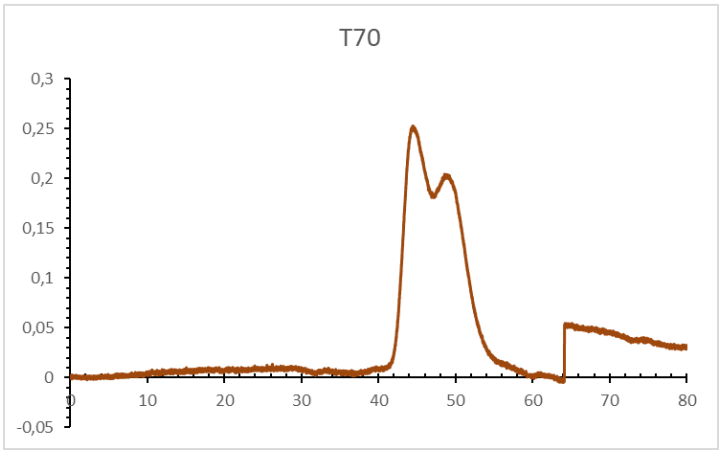
T70
0,3
0,25
0,2
0,15
0,1
0,05
0
-0,05
0
10
20
30
40
50
60
70
80

Appendix

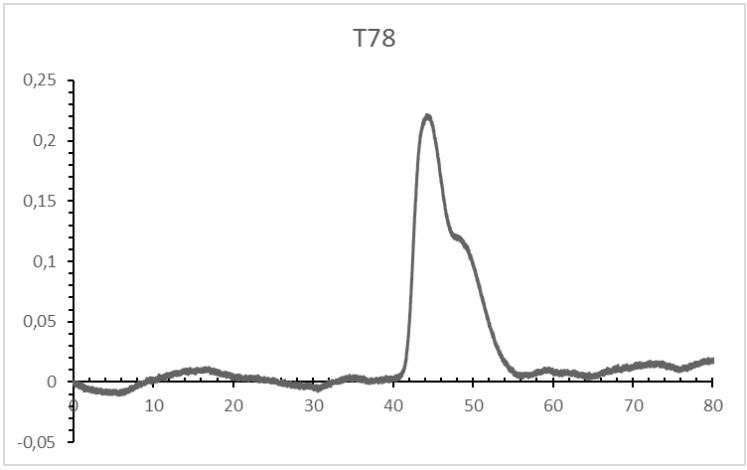
T78
0,25
0,2
0,15
0,1
0,05
0
-0,05
0
10
20
30
40
50
60
70
80

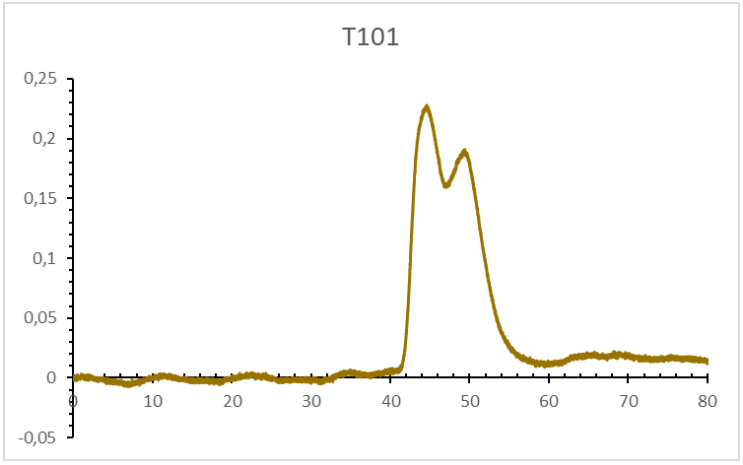
T101
0,25
0,2
0,15
0,1
0,05
0
-0,05
0
10
20
30
40
50
60
70
80

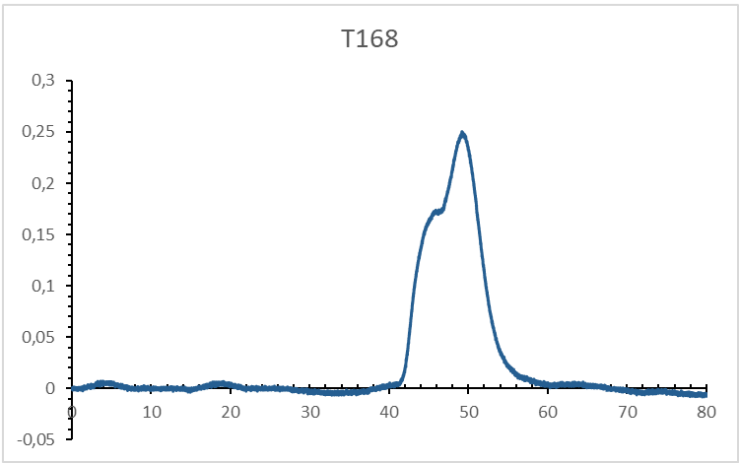
T168
0,3
0,25
0,2
0,15
0,1
0,05
0
-0,05
0
10
20
30
40
50
60
70
80